UNIVERSIDAD AUTÓNOMA DE NUEVO LEÓN

FACULTAD DE INGENIERÍA MECÁNICA Y ELÉCTRICA

ANALYSIS OF CLOSED - LOOP THERAPY IN TYPE II DIABETES

POR

ING. ANA ALEJANDRA OLAY BLANCO

EN OPCIÓ N AL GRADO DE

MAESTRÍA EN CIENCIAS DE LA INGENIERÍA ELÉCTRICA

JULIO, 2018

UNIVERSIDAD AUTÓNOMA DE NUEVO LEÓN

FACULTAD DE INGENIERÍA MECÁNICA Y ELÉCTRICA

SUBDIRECCIÓN DE ESTUDIOS DE POSGRADO

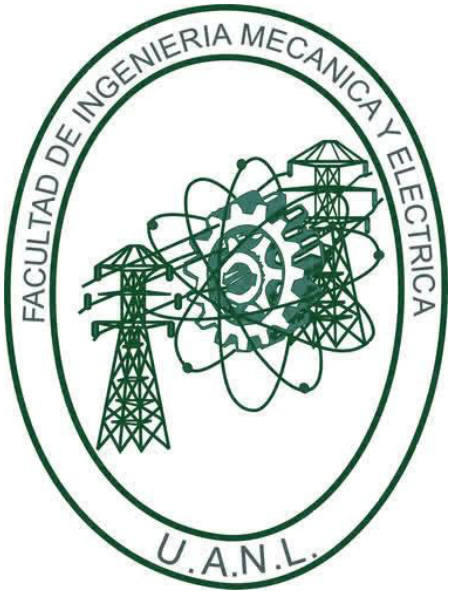

ANALYSIS OF CLOSED - LOOP THERAPY IN TYPE II DIABETES

POR
ING. ANA ALEJANDRA OLAY BLANCO

EN OPCIÓ N AL GRADO DE
MAESTRÍA EN CIENCIAS DE LA INGENIERÍA ELÉCTRICA

DIRECTORA DE TESIS
DRA. GRISELDA QUIROZ COMPEÁN

SAN NICOLÁS DE LOS GARZA, NUEVO LEÓN, MÉXICO **JULIO, 2018**

UANL

FACULTAD DE INGENIERÍA MECÁNICA Y ELECTRICA

UNIVERSIDAD AUTÓNOMA DE NUEVO LEÓN

FACULTAD DE INGENIERÍA MECÁNICA Y ELÉCTRICA

SUBDIRECCIÓN DE ESTUDIOS DE POSGRADO

Los miembros del Comité de Tesis recomendamos que la Tesis "Analysis of closed-loop therapy in type II diabetes" realizada por el alumno(a) Ana Alejandra Olay Blanco, con número de matrícula 1488730, sea aceptada para su defensa como opción al grado de Maestría en Ciencias de la Ingeniería Eléctrica.

El Comité de Tesis

Dra. Griselda Quiroz Compeán
Director

Dr. Luis Martín Torres Treviño
Revisor

Dra. Claudia Patricia Flores Gutiérrez
Revisor

Vo. Bo.

Dr. Simón Martínez Martínez
Subdirector de Estudios de Posgrado

San Nicolás de los Garza, Nuevo León, 12 de julio de 2018

Acknowledgement

I am so glad to thank my family, specially to my parents who are my inspiration to work in this project. Mom, Dad, Angie, Marce: thanks for your support through all my life and to encourage me to go further with my studies. I love you all and I am profoundly grateful with you. I am also so grateful to J. Manuel Zamora, thank you for helping me out with the computing that I needed for this research, for all your academic support and your love through all this time but mainly for being part of the most important project in this life, I love you so much. To all of you: I cannot find the words to let you all know how much you mean to me.

I'd also like to thank Dra. Griselda Quiroz Compeán. Thanks for letting me work with you again, for all the new knowledge you lend me and your patience, also for your support and guidance with this project. At this point, I extend my acknowledgement to the Consejo Nacional de Ciencia y Tecnología (CONACYT) for the financial support they brought to this project, with the grant C.B. 2013 - 220187 and scholarship 448599.

To all my friends, thanks for the chatting and your support. To the professors of this program, I thank you for the knowledge I got during the courses. Special thanks to Dr. Juan Ángel Rodríguez Liñán and Dr. Jesús Emmanuel Goméz Correa, for the work done altogether and the academic guidance you gave me. Also thanks to the committee members (Dr. Luis M. Torres Treviño and Dra. Claudia Patricia Flores Gutiérrez) for your time and your comments towards this work.

Last but not least, I'd like to thank God for allowing me to get to this chapter in my life, for everything I learnt and the persons I met.

To my beloved family and my dearest one...

And to God...

Audere est facere.

Contents

Abstract

Diabetes mellitus is a worldwide pandemic, which prevalence has increased in the last years. This disease is mainly characterized by increased basal blood glucose levels, called hyperglycemia. According to the causes, diabetes mellitus can be classified in three types: i) gestational, related to hormonal and metabolic imbalances during pregnancy, ii) type 1 diabetes, which is an immune disease characterized by the progressive death of pancreatic βcells, that produce insulin, the principal hormone in glucose metabolism; and iii) type 2 diabetes, which is a metabolic disease characterized by dysfunction use and production of insulin. Type 2 diabetes mellitus is the most recurrent one, including more than 95 % of the clinical cases. Some recent studies have shown that the implementation of the automation of insulin dosage for type 2 diabetes patients can improve their treatment. Based on this problem, the main objective of this thesis is to develop a methodology to analyze the viability of having a closed-loop therapy for type 2 diabetes mellitus. The study includes the revision on two mathematical models of blood glucose metabolism useful to synthesize control schemes. Moreover, a methodology to personalize this kind of models based on metabolic data from continuous glucose monitoring of type 2 diabetic patients is presented. After that, the analysis of some characteristics of the models, their role in closed-loop therapy and a case of study using a conventional control scheme are presented.

Keywords:
Diabetes, *glucose metabolism modeling*, *closed-loop therapy*, *virtual patient*

Resumen

La diabetes mellitus es una pandemia mundial, la cual ha incrementado su prevalencia en los últimos años. Esta enfermedad es principalmente caracterizada por el aumento de los niveles basales de glucosa en sangre, llamado hiperglicemia. De acuerdo a las causas, la diabetes mellitus puede ser clasificada en tres tipos: i) gestacional, relacionada con desbalances hormonales y metabólicos durante el embarazo, ii) tipo 1, la cual es una enfermedad autoinmune caracterizada por la muerte progresiva de las células beta pancreáticas, las cuales se encargan de producir insulina, la hormona principal en el metabolismo de glucosa; y iii) tipo 2, la cual es una enfermedad metabólica caracterizada por el uso y producción disfuncional de la insulina. La diabetes mellitus tipo 2 es la más recurrente, incluyendo más del 95 % de casos clínicos. Algunos estudios recientes han mostrado que la implementación de la automatización en la dosificación de insulina para pacientes con diabetes tipo 2 puede mejorar su tratamiento. Basándose en este problema, el principal objetivo de esta tesis es desarrollar una metodología para analizar la viabilidad de tener una terapia en lazo cerrado para diabetes tipo 2. El estudio incluye la revisión de dos modelos matemáticos del metabolismo de glucosa en sangre de gran utilidad para la síntesis de esquemas de control. Además, se presenta una metodología para personalizar este tipo de modelos basados en información metabólica proveniente del monitoreo continuo de glucosa en pacientes con diabetes tipo 2. Después, se muestra el análisis de algunas características de los modelos, su rol en la terapia de lazo cerrado y un caso de estudio usando un control convencional.

Palabras clave:
Diabetes, modelado del metabolismo de glucosa, terapia en lazo cerrado, paciente virtual

Chapter 1

Introduction

1.1 Health problem

According to the latest reports made by the International Diabetes Federation (IDF), in 2017 there were 425 million people around the world living with any type of diabetes, they expect that this figure increases up to 629 million people in 2045. According to the causes, diabetes mellitus can be classified in three types: i) gestational, related to hormonal and metabolic imbalances during pregnancy, ii) type 1 diabetes (T1DM), which is an immune disease characterized by the progressive death of pancreatic β-cells, that produce insulin, the principal hormone in glucose metabolism; and iii) type 2 diabetes (T2DM), which is a metabolic disease characterized by dysfunction use and production of insulin. The one with more prevalence is T2DM, in higher income countries the total of adults that suffer from diabetes, near the 91% have T2DM, this is not considering the undiagnosed patients [1]. Observing the data by regions, in North America and the Caribean 13% of the population, between 20 – 79 years old, is affected by some type of diabetes. Also this region has the most elevated prevalence compared to the other regions. In Mexico, according to the 2016 National Health and Nutrition Examination Survey (ENSANUT, by its acronym in Spanish), the prevalence of diabetes in people older than 20 years old in the country was 7.2% back in 2006 and 9.4% ten years later. Only 87.8% of the affected survey respondents said that they take a treatment to control this illness; from the total of the polled diabetic patients, 46.4% do not take preventive actions to delay or avoid diabetic derived

complications [2].

Due to the impact of T2DM in public health, many methodologies have been developed to help medicine to have a better understanding this illness; one of them is mathematical modeling. Depending on the purpose and the biological process that is wanted to reproduce, the mathematical models can be classified as clinical and non-clinical [3]. Clinical models are constructed by simple mathematical structure and they emulate the clinical data considering just the systemic description of the human body ([4], [5], [6]); meanwhile the non-clinical models are composed by complex mathematical structure and they are based in the nature and the mechanistic description of the physiological processes that contribute to the glucose metabolism ([7], [8], [9]). The clinical models are used in diagnosis tools and they are focused in insulin sensitivity and secretion, glucose effectiveness and beta cells functionality [10]. These have been developed by intravenous glucose tolerant test (IVGTT), placing minimal models and their modifications [5]. Also, there are models that focus in the illness progression based in beta cells function, making them to be commonly used for T2DM models [11].

Regarding non-clinical models, the approach is to model the physiological processes of the main organs related to the glucose metabolism, to analyze the way these organs interact among each other. Generally, in physiological modeling, it is proposed to divide the human body into compartments, where each one of them represents an organ and it is analyzed the time variance of the glucose concentration in each compartment. For example, the model proposed by Tiran *et al.* describes the glucose and insulin dynamics in the main organs involved in the process: brain, heart, stomach, liver, kidneys and peripheral tissues (muscle and lipid) and their interconnection through circulatory system [10]. Starting from the latter, Sorensen proposed another model detailing the glucose metabolism and insulin and glucagon regulation in the same eight organs and tissues involved in the process [8]. By making modifications to the model proposed by Sorensen, it is possible to adapt it in order to describe type 1 and type 2 diabetes mellitus, just as it was proposed by Alvehag and Martin, who modeled the pancreas as a separated compartment and modified the model for it to be able to handle different oral glucose supplies [8]. Recently, Vahidi *et al.* presented a new modification to

Sorensen's model, in which, by solving optimization problems using clinical data, they obtained the parametric estimation to model T2DM [9].

Non-clinical models allow the prediction of the dynamic behavior of glucose metabolism, which can be used to improve diabetes treatments. For example, in real practice insulin dosage is made by empiric rules that the diabetes specialist defines in function of the knowledge of the patients' metabolism. The use of mathematical models would allow calculating personalized doses for each patient due its theoretical origin. This leads to the development of new therapies to enhance the life quality of the patients, therefore it heads to automation schemes for insulin dosage. This kind of therapies get developed in a conjunction of mathematical models and controllers, where the main objective is to reduce the variations of the glucose concentration and to keep it in a normal range (normoglycemia) [10], considering the different factors involved in glucose regulation (diet, exercise and metformin or insulin supply). An automated system for diabetes control requires three main parts: a blood glucose measuring system, a control system that works with a measured input of glucose and that generates an output response and a supply system for insulin release [11].

Nowadays, insulin dosage therapies have a major focus on T1DM patients. From the different kinds of control algorithms that have been studied, model predictive control (MPC) is the one that has have more development in this area; with this control, the action is gathered by solving an optimal control problem in a finite horizon for each sample point, using the actual state of the system as initial state [11]. Recently, Najafabadi and Shahrokhi performed a study where they compared a linear model with a non-linear model, both using a MPC, they concluded that the non-linear model presented better results in robustness in presence of noise in the measurements [10]. Betting for a more personalized control, Zavitsanou *et al.* proposed a model for insulin delivery for T1DM patients, also based in a MPC. This control is based in a state estimator and an optimization problem solution for an open-loop for patient-specific therapy. If the patient's data is limited, this control strategy can be modified in order to make an approximation [12].

As told before, the usage of the existent models and controllers opens the development of new tools for the improvement in diabetes treatments. Virtual patients (or *in silico* models) and artificial pancreas are the tools that have a major impact at the moment. An example of this is the virtual patient simulator, based on plasmatic concentrations and glucose and insulin fluxes [13]. It was done by the University of Virginia along with the University of Padova, and it was approved by the U.S. Food and Drug Administration (U.S. FDA); this became a tool that substitutes preclinical trials performed in animals [14]. Another simulator that has been developed by the Illinois Institute of Technology as an educative tool is GlucoSim [15].

Regarding the artificial pancreas, Medtronic® has developed a hybrid closed-loop system that has been approved by the U.S. FDA [16]. This system adjusts the insulin delivery automatically, the only interaction that it has with the patient is the input of the carbohydrates intake (CHO intake) and the postprandial blood glucose measurement [17].

Due to most of models and controllers are designed for T1DM and by looking at the reported numbers, the goal of this research is to focus in T2DM because it is the one that needs more attention and development of prediction and prevention tools.

1.2 Problem definition

Even though treatments based on hypoglycemic drugs and long-acting insulin in T2DM patients achieve the lowering of the blood glucose levels, it has been observed that in some cases it is not enough to get them to the normoglycemic levels. Because of that, it is proposed that a closed-loop control scheme handles insulin release, in order to reach normal blood glucose levels.

1.3 Hypothesis

The use of personalized models and closed-loop control schemes allows enhancing T2DM treatment by considering the feedback of blood glucose concentration

and insulin as control input signal, just as perturbations by food intake.

1.4 Objectives

1.4.1 General objective

The main objective of this thesis is to analyze the convenience of the use of closed-loop control schemes in T2DM therapies, considering perturbations performed by carbohydrate intake and insulin supply.

1.4.2 Specific objectives

The specific objectives of this research are:

1. Analysis of compartmental mathematical models of glucose metabolism considering models of carbohydrate intake.
2. Parameter adjustment of a mathematical model of the glucose metabolism in order to adapt it to data of a T2DM patient from continuous glucose monitoring systems.
3. Design of a feedback control scheme for the supply of insulin.

1.5 Methodology

The methodology used to develop this research is divided in three stages. The first stage considered the data analysis of an experimental protocol of the blood glucose concentration monitoring of a study subject where the daily carbohydrate intake (CHO intake) is recorded as well. The second stage was the mathematical modeling interested in getting an algorithm that reproduces the glucose concentration patterns obtained in the previous experimental protocol. In this stage, a sensitivity analysis was proposed to make the parametric adjustment of the mathematical model. In the third stage a control scheme was designed in order to implement a closed-loop control for insulin and metformin supply.

Chapter 2

Modeling glucose metabolism in type 2 diabetes mellitus

In order to model the glucose metabolism of a T2DM patient, it is necessary to previously understand how the glucose metabolism of a healthy person works. Then, by knowing how the illness affects the metabolism changes can be made. In this section, two models that describe the glucose-insulin dynamics are presented. The first one, called meal-glucose-insulin model, considers the main processes for glucose metabolism considering meal intake and the second one, which is called physiological model, considers the mass balance between the main organs involved in this process. Both of the models are based on compartmental modeling. Also, a gastric emptying model is presented in order to adapt it to the physiological model to represent the carbohydrate intake.

2.1 Mathematical models background

The mathematical model of T2DM commonly focuses in how the beta-cells work; this is because in this illness their function is affected by the change in their mass. In 2000, Topp *et al.* proposed a three equation model that described the dynamics on the quantification of the beta-cells and the evolution of the basal blood glucose and insulin. This model was based in the production and utilization of the glucose and insulin, as well as, the born and death of the beta-cells. Because of

the different time that their action has, it is divided in a fast system (glucose and insulin system) and a slow system (beta-cell system) [18].

Based on the models by De Gaetano and Arino [19], Silber *et al.* proposed a model by analyzing simultaneous measurements of glucose concentration, glucose concentration with tracers and insulin concentration, this because glucose and insulin have an interaction in the same system at the same time. They also incorporated a control mechanism to regulate glucose production, insulin secretion and glucose absorption [20]. In order to do the modeling, they used intravenous glucose provocation in healthy and T2DM patients. This model is of interested for the data analysis for the development of hypoglycemic drugs and for the optimization of protocol design. Recently, Vahidi *et al.* presented improvements to their previous T2DM model (based on the healthy patient model by Sorensen), where the input signal was limited to glucose injection [9]. The previous issue was solved by adding a model of gastric glucose absorption such that variations in plasmatic glucose concentration and food intake are considered. They also added a model that represented the produced incretins in the gastrointestinal tract with its hormonal effect that elevated the pancreatic insulin production [21]. In 2017, Othman *et al.* proposed a proportional-derivative model of endogenous insulin secretion and insulin dynamics to track T2DM progression [22]. This model is of interest for the low cost methodologies for the analysis of the pathogenesis of T2DM because this model describes the different stages of it.

Due to the available information and the technology evolution in the last decades, new methods can be implemented in modeling; a clear example is the use of artificial intelligence [23]. Some of the latest applications of this technology are in image analysis, drug design, biochemical analysis and diagnostic systems, where the later has a major development in diabetes. In 2012, Karan *et al.* presented the initial results of client-server architecture for mobile devices. This architecture analyzes some certain patient data and can tell if the presented characteristics are signal of a possibility of developing diabetes [24]. In this research, they use a multilayer perceptron artificial neural network that consisted of 11 inputs, one hidden layer and two outputs; it was trained with 228 healthy patient data and 228 diabetic patients. The required data to make the diagnosis are: age, physical

activity, pregnancy, diabetes in the family, body mass index, skin fold thickness, cholesterol level, diastolic blood pressure, 2-hour serum insulin, pedigree of diabetes and blood glucose concentration.

Most specifically for T2DM, Wang *et al.* developed a study to evaluate the risk of T2DM in rural adults [25]. They implemented an artificial neural network model (ANN) and a multivariate logistic regression (MLR) model. It was trained with the random selection of the 75% out of 8640 subjects and there were 17 considered variables based in demographic, anthropometric and lifestyle data. The results showed a more exact prediction with the ANN model than with the MLR model, the presented prevalence rate in the training was 8.66% for the ANN model and 9.21% for the MLR model. There is a technology called "electronic nose", which bases on simulating the mammal sense of smell with sensors and it allows repetitively measurement gathering of mixtures of scents for identification and classification by ANN [26]. With this technology, El *et al.* developed a predictive model to predict T2DM based in urine samples of healthy and diabetic patients [27].

Conventional treatment for T2DM is based in hypoglycemic drugs, where metformin is the most commonly taken. Therefore, it is important to know what the effects it has in T2DM patients. In 2004, Lee *et al.* ran an experiment to model the effects of glucose lowering by metformin in healthy patients [28]. Later, Sun *et al.* modeled metformin pharmacokinetics and pharmacodynamics in T2DM patients, considering the model proposed in 2010 by Vahidi *et al.* The main modeled effects were the increment on the consumption of the intestinal glucose rate, the decrement on the hepatic glucose output and the increment on the muscular cells and adipocytes uptake [29]. Based on metformin pharmacokinetics and mass balance, Chakraborty *et al.* proposed a deterministic model which can predict the time history concentration in the stomach, intestine and periphery areas [30].

Some studies have been made in order to know the effects of the early insulin administration in T2DM patients, added to an antihyperglycemic drug therapy. Results have shown that the percentages of glycosylated hemoglobin (HbA1c) are lower, just as the risks of mortal diabetes complications [31]. Nowadays new tests are being developed in order to find more effective therapies, one of them is the

insulinization therapy, which bases in continuous infusion of subcutaneous insulin. Lian *et al.* reported eight experiments, one of them using the insulinization therapy. It showed better results out of all the experiments by reducing the index of patients that used oral antihyperglucemic drugs, also by reducing the time to get to an optimal glycemic level and the severe incidence of hypoglycemia [32].

In order to make a more accurate model of diabetes, it is important to know the effect of the nutrients contained on the food that is ingested. It was not found any work focused in glucose absorption coming from a different nutrient source than carbohydrates. Besides this issue, there are many models that consider carbohydrates absorption as an external source of glucose, such as Hovorka [33], Cobelli [34] and Lehmann [35].

In this thesis, we are interested in mathematical models useful to study closed loop therapy in T2DM, Thus we select two compartmental models. The first one is the proposed by Dalla Man *et al* in 2007 [34], and the second one is the proposed by Sorensen in 1985 [7]. Both models are described in the next sections.

2.2 Meal - glucose - insulin model

The meal - glucose - insulin model was proposed by Dalla Man *et al.* in [34], which is divided in six subsystems. The first one is the glucose subsystem, which describes the mass of glucose in plasma and rapidly equilibrating tissues ($G_p(t)$) and the mass of glucose in slowly equilibrating tissues ($G_t(t)$). This subsystem takes endogenous ($EGP(t)$) and exogenous ($Ra(t)$) sources of glucose, as well as the insulin-dependent ($U_{id}(t)$) and -independent ($U_{ii}(t)$) glucose utilization and renal excretion ($E(t)$):

$$\frac{dG_p(t)}{dt} = EGP(t) + Ra(t) - U_{ii}(t) - E(t) - k_1 G_p(t) + k_2 G_t(t) \tag{2.1}$$

$$\frac{dG_t(t)}{dt} = -U_{id}(t) + k_1 G_p(t) - k_2 G_t(t) \tag{2.2}$$

where k_1 and k_2 (min^{-1}) are the rate parameters of distribution, and the equations that describe the processes involved in the modeling of $G_p(t)$ and $G_t(t)$ are described bellow:

$$
\begin{aligned}
EGP(t) &= k_{p1} - k_{p2}G(t) - k_{p3}I_d(t) - k_{p4}I_{po}(t) && (2.3)\\
Ra(t) &= \frac{f\,k_{abs}Q_{gut}(t)}{BW} && (2.4)\\
U_{ii}(t) &= F_{cns} && (2.5)\\
E(t) &= \begin{cases} k_{e1}[G_p(t) - k_{e2}], & \text{if } G_p > k_{e2} \\ 0 & \text{if } G_p \leq k_{e2} \end{cases} && (2.6)\\
U_{id}(t) &= \frac{V_m(X(t))G_t(t)}{K_m(X(t)) + G_t(t)} && (2.7)\\
V_m(X(t)) &= V_{m0} + V_{mx}X(t) && (2.8)\\
K_m(X(t)) &= K_{m0} && (2.9)
\end{aligned}
$$

where k_{p1} (mg/kg/min) is the extrapolated $EGP(t)$ at zero glucose and insulin, k_{p2} (min^{-1}) is the rate of liver glucose effectiveness, k_{p3} (mg/kg/min per pmol/l) is the parameter governing amplitude of insulin action on the liver, k_{p4} (mg/kg/min per pmol/l) is the parameter governing amplitude of portal insulin action on the liver, I_{po} (pmol/kg) is the amount of insulin in the portal vein. f (dimensionless) is the fraction of intestinal absorption that actually appears in plasma, k_{abs} (min^{-1}) is the constant rate of intestinal absorption and BW (kg) is the body weight. F_{cns} (mg/kg/min) is the constant glucose uptake by the brain and erythrocytes, k_{e1} (min$^-$1) is the glomerular filtration rate, k_{e2} (mg/kg) is the renal threshold of glucose. $V_m(X(t))$ and $K_m(X(t))$ (mg/kg/min per pmol/l) are functions that depend on the insulin in the interstitial fluid.

The blood glucose concentration $G(t)$ is the relationship of appearance of the mass of glucose in plasma $G_p(t)$ in a certain distribution volume V_G, this is described as follows:

$$G(t) = \frac{Gp(t)}{V_G} \tag{2.10}$$

The second subsystem describes the mass of the insulin in liver ($I_l(t)$) and in blood ($I_p(t)$):

$$\frac{dI_l(t)}{dt} = -(m_1 + m_3(t))I_l(t) + m_2 I_p(t) + S(t) \tag{2.11}$$

$$\frac{dI_p(t)}{dt} = -(m_2 + m_4)I_p(t) + m_1 I_l(t) \tag{2.12}$$

where m_1, m_2, $m_3(t)$, m_4 (min^{-1}) are rate parameters of distribution and $S(t)$ (pmol/L/min) is the insulin secretion and is a function described as:

$$S(t) = \gamma I_{po}(t), \tag{2.13}$$

where $I_{po}(t)$ (pmol/kg) is the amount of insulin in the portal vein, which change respect time is described in Equation (2.24) and γ (min^{-1}) is the rate of transference between the portal vein and the liver; $m_3(t)$ is described as:

$$m_3(t) = \frac{HE(t)m_1}{1 - HE(t)} \tag{2.14}$$

$$HE(t) = -m_5 S(t) + m_6 \tag{2.15}$$

where $HE(t)$ (dimensionless) is the hepatic extraction of insulin.

The blood insulin concentration $I(t)$ can be described in a similar way than blood glucose concentration, where the plasmatic mass I_p of insulin is delivered within a distribution volume V_I, this process is described as follows:

$$I(t) = \frac{Ip(t)}{V_I} \tag{2.16}$$

$EGP(t)$ in Equation 2.3 requires the dynamics of insulin described in the next equations:

$$\frac{dI_d(t)}{dt} = -k_i[I_d(t) - I_1(t)] \tag{2.17}$$
$$\frac{dI_1(t)}{dt} = -k_i[I_1(t) - I(t)] \tag{2.18}$$

where $I_d(t)$ is a delayed insulin signal, $I_1(t)$ is an auxiliary variable of $I_d(t)$ and k_i (min^{-1}) is the rate parameter accounting for delay between insulin signal and insulin action. Since this model considers meal intake, the fourth subsystem describes glucose rate of appearance due to this disturbance. The process considers that glucose enters first in a solid phase and then it goes into a liquid phase in stomach to finish the absorption in the intestine.

$$\frac{dQ_{sto1}(t)}{dt} = -k_{gri}Q_{sto1}(t) + Dd(t) \tag{2.19}$$
$$\frac{dQ_{sto2}(t)}{dt} = -k_{empt}(Q_{sto})Q_{sto2}(t) + k_{gri}Q_{sto1}(t) \tag{2.20}$$
$$\frac{dQ_{gut}(t)}{dt} = -k_{abs}Q_{gut}(t) + k_{empt}(Q_{sto})Q_{sto2}(t) \tag{2.21}$$
$$Q_{sto} = Q_{sto1}(t) + Q_{sto2}(t),$$

where Q_{sto1} and Q_{sto1} (mg) are the masses of glucose in stomach, one in solid phase and other in liquid phase. Q_{gut} (mg) is the mass of glucose in the intestine. k_{gri} (min^{-1}) is the rate of grinding, k_{abs} (min^{-1}) is the rate of intestinal absorption and $k_{empt}(Q_{sto})$ (min^{-1}) is the rate of gastric emptying described by:

$$\begin{aligned} k_{empt}(Q_{sto}) &= k_{min} + \frac{k_{max} - k_{min}}{2}\{tanh\left[\frac{5}{2D(1-b)}(Q_{sto}(t) - bD)\right] \\ &- tanh\left[\frac{5}{2Dc}(Q_{sto}(t) - cD)\right] + 2\} \end{aligned} \tag{2.22}$$

where k_{min} (min^{-1}) is the rate at which the stomach contains the minimum amount of ingested glucose, k_{max} (min^{-1}) is the rate at which the stomach contains the

whole amount of ingested glucose, D (mg) is the amount of ingested glucose, b is the percentage of the dose for which k_{empt} decreases at (k_{max}-k_{min})/2, and c is the percentage of the dose for which k_{empt} is back to (k_{max}-k_{min})/2.

The fifth subsystem is the glucose utilization ($X(t)$):

$$\frac{dX(t)}{dt} = -p_{2U}X(t) + p_{2U}[I(t) - I_b] \tag{2.23}$$

where I_b (pmol/L) is the basal insulin concentration and p_{2U} (min^{-}1) is the rate constant of insulin action of the peripheral glucose utilization.
Finally, the last subsystem describes insulin secretion:

$$\frac{dI_{po}(t)}{dt} = -\gamma I_{po}(t) + S_{po}(t) \tag{2.24}$$

$$\frac{dY(t)}{dt} = \begin{cases} -\alpha[Y(t) - \beta(G(t) - h)], \text{ if } \beta(G(t) - h) \geq -S_b \\ -\alpha Y(t) - \alpha S_b, \text{ if } \beta(G(t) - h) < -S_b \end{cases} \tag{2.25}$$

where $Y(t)$ (mg/dl) is the insulin release threshold, h (mg/dl) is the threshold level of glucose above which β-cells initiate to produce new insulin, α (min^{-1}) is the delay between glucose signal and insulin secretion, β (pmol/kg/min) is the pancreatic responsivity to glucose, $S_{po}(t)$ (pmol/kg) is the insulin secretion of the portal vein and S_b (pmol/kg) is the basal insulin secretion.

In order to adapt this model to describe the glucose-insulin dynamics of a T2DM patient, the structure of the model stays the same but the parameters change. The parameters used to adapt it to a T2DM patient can be seen in Table 2.1.

Parameter	Value	Parameter	Value
V_G	1.49 dl/kg	k_{max}	0.0465 min^{-1}
k_1	0.042 min^{-1}	k_{min}	0.0076 min^{-1}
k_2	0.071 min^{-1}	k_{abs}	0.023 min^{-1}
V_I	0.04 l/kg	k_{gri}	0.0465 min^{-1}
m_1	0.379 min^{-1}	f	0.092
m_2	0.673 min^{-1}	b	0.68
m_4	0.269 min^{-1}	c	0.00023 mg^{-1}
m_5	0.0526 $min\ kg/pmol$	k_{p1}	3.09 $mg/kg/min$
m_6	0.8118	k_{p2}	0.0007 min^{-1}
HE_b	0.6	k_{p3}	0.005 $mg/kg/min$ per $pmol/l$
γ	0.5 min^{-1}	k_{e1}	0.0007 min^{-1}
k_{p4}	0.0786 $mg/kg/min$ per $pmol/kg$	k_i	0.0066 min^{-1}
F_{cns}	1 $mg/kg/min$	V_{m0}	4.65 $mg/kg/min$
V_{mx}	0.034 $mg/kg/min$ per $pmol/l$	K_{m0}	466.21 mg/kg
p_2U	0.084 min^{-1}	K	0.99 $pmol/kg$ per mg/dl
α	0.013 min^{-1}	β	0.05 $pmol/kg/min$ per mg/dl
k_{e2}	269 mg/kg		

Table 2.1: Parameters used in the meal-glucose-insulin model for T2DM.

2.3 Physiological model for type 2 diabetes mellitus

Based on the healthy human body model proposed by Sorensen [7], Vahidi *et al.* developed a model for T2DM by using available clinical data [9]. This model describes the glucose dynamics in brain, heart, stomach, liver, kidneys and peripheral tissues. This model can be used to predict deficiencies in processes such as pancreatic insulin production, impaired hepatic regulatory effect on glucose concentration and low peripheral glucose uptake. This model is divided into three subsystems: glucose subsystem, insulin subsystem and glucagon subsystem.

The glucose subsystem is described with eight differential equations of each organ and three differential equation of metabolic rates, as shown below:

$$\frac{dG_{BV}}{dt} = \left[Q_B^G(G_H - G_{BV}) - \frac{V_{BI}^G}{T_B^G}(G_{BV} - G_{BI})\right]/V_{BV}^G \quad (2.26)$$

$$\frac{dG_{BI}}{dt} = \left[\frac{V_{BI}^G}{T_B^G}(G_{BV} - G_{BI}) - r_{BGU}\right]/V_{BI}^G \quad (2.27)$$

$$\frac{dG_H}{dt} = \left[Q_B^G G_{BV} + Q_L^G G_L + Q_K^G G_K + Q_P^G G_{PV} - Q_H^G G_H - r_{RBCU}\right]/V_H^G \quad (2.28)$$

$$\frac{dG_G}{dt} = \left[Q_G^G(G_H - G_G) - r_{GGU}\right]/V_G^G \quad (2.29)$$

$$\frac{dG_L}{dt} = \left[Q_A^G G_H + Q_G^G G_G - Q_L^G G_L + r_{HGP} - r_{HGU}\right]/V_L^G \quad (2.30)$$

$$\frac{dG_K}{dt} = \left[Q_K^G(G_H - G_K) - r_{KGE}\right]/V_K^G \quad (2.31)$$

$$\frac{dG_{PV}}{dt} = \left[Q_P^G(G_H - G_{PV}) - \frac{V_{PI}^G}{T_P^G}(G_{PV} - G_{PI})\right]/V_{PV}^G \quad (2.32)$$

$$\frac{dG_{PI}}{dt} = \left[\frac{V_{PI}^G}{T_P^G}(G_{PV} - G_{PI}) - r_{PGU}\right]/V_{PI}^G \quad (2.33)$$

$$\frac{dM_{HGP}^I}{DT} = 0.04(M_{HGP}^{I\infty} - M_{HGP}^I) \quad (2.34)$$

$$\frac{df}{dt} = 0.0154\left[\left(\frac{2.7tanh[\frac{0.39\Gamma}{\Gamma^B} - 1]}{2}\right) - f\right] \quad (2.35)$$

$$\frac{dM_{HGU}^I}{DT} = 0.04(M_{HGU}^{I\infty} - M_{HGU}^I) \quad (2.36)$$

where G_{BV} (mg/dl) is the brain vascular glucose concentration, G_{BI} (mg/dl) is the brain interstitial glucose concentration, G_H (mg/dl) is the heart vascular concentration, G_G (mg/dl) is the gut glucose concentration, G_L (mg/dl) is the liver glucose concentration, G_K (mg/dl) is the kidney glucose concentration, G_{PV} (mg/dl) is the peripheral vascular glucose concentration, G_{PI} (mg/dl) is the peripheral interstitial glucose concentration, M_{HGP}^I is the hepatic glucose production metabolic rate, f is a function related to the glucagon effect in the hepatic glucose production rate and M_{HGU}^I is the hepatic glucose production metabolic rate. Q (l/min) represents the vascular blood flow rate of the respective organ and V (l) represents the volumes of the respective organ.

The glucose subsystem has a set of metabolic rates which are described below:

$$r_{BGU} = 70 \tag{2.37}$$

$$r_{RBCU} = 10 \tag{2.38}$$

$$r_{GGU} = 20 \tag{2.39}$$

$$r_{PGU} = M^{I}_{PGU} M^{G}_{PGU} r^{B}_{PGU} \tag{2.40}$$

$$r^{B}_{PGU} = 35 \tag{2.41}$$

$$M^{I}_{PGU} = 2.788 + 1.915 tanh\left[0.619\left(\frac{I_{PF}}{I^{B}_{PF}} - 3.719\right)\right] \tag{2.42}$$

$$M^{G}_{PGU} = \frac{G_{PF}}{G^{B}_{PF}} \tag{2.43}$$

$$r_{HGP} = M^{I}_{HGP} M^{G}_{HGP} M^{\Gamma}_{HGP} r^{B}_{HGP} \tag{2.44}$$

$$r^{B}_{HGP} = 35 \tag{2.45}$$

$$M^{I\infty}_{HGP} = 0.691 - 0.626 tanh\left[0.998\left(\frac{I_L}{I^{B}_{L}} - 1.54\right)\right] \tag{2.46}$$

$$M^{G}_{HGP} = 1.42 - 1.41 tanh\left[0.62\left(\frac{G_L}{G^{B}_{L}} - 0.497\right)\right] \tag{2.47}$$

$$M^{\Gamma}_{HGP} = 2.7 tanh\left[0.39\frac{\Gamma}{\Gamma^{B}}\right] - f \tag{2.48}$$

$$r_{HGU} = M^{I}_{HGU} M^{G}_{HGU} r^{B}_{HGU} \tag{2.49}$$

$$r^{B}_{HGU} = 20 \tag{2.50}$$

$$M^{I\infty}_{HGU} = 0.845 + 0.624 tanh\left[0.894\left(\frac{I_L}{I^{B}_{L}} - 0.715\right)\right] \tag{2.51}$$

$$M^{G}_{HGU} = 2.201 + 2.232 tanh\left[1.883\left(\frac{G_L}{G^{B}_{L}} - 1.319\right)\right] \tag{2.52}$$

$$r_{KGE} = \begin{cases} 71 + 71 tanh\left[0.11\left(G_K - 460\right)\right], \text{ if } 0 \leq G_K \leq 460 \\ -330 + 0.872 G_K, \text{ if } G_K \geq 460 \end{cases} \tag{2.53}$$

In a similar arrangement, the insulin subsystem is described with seven differential equations and three differential equations for an insulin inhibitor.

$$\frac{dI_B}{dt} = \left[Q_B^I(I_H - I_B)\right]/V_B^I \tag{2.54}$$

$$\frac{dH_H}{dt} = \left[Q_B^I I_B + Q_L^I I_L + Q_K^I I_K + Q_{PV}^I I_{PV} - Q_H^I I_H\right]/V_H^I \tag{2.55}$$

$$\frac{dI_G}{dt} = \left[Q_G^I(I_H - I_G)\right]/V_G^I \tag{2.56}$$

$$\frac{dH_L}{dt} = \left[Q_A^I I_H + Q_G^I I_G - Q_L^I I_L + r_{PIR} - r_{LIC}\right]/V_L^I \tag{2.57}$$

$$\frac{dI_K}{dt} = \left[Q_K^I(I_H - I_K) - r_{KIC}\right]/V_K^I \tag{2.58}$$

$$\frac{dI_{PV}}{dt} = \left[Q_P^I(I_H - I_{PV}) - \frac{V_{PI}^I}{T_P^I}(I_{PV} - I_{PI})\right]/V_{PV}^I \tag{2.59}$$

$$\frac{dI_{PI}}{dt} = \left[\frac{V_{PI}^I}{T_P^I}(I_{PV} - I_{PI}) - r_{PIC}\right]/V_{PI}^I \tag{2.60}$$

$$\frac{dm}{dt} = Km_0 - Km + \gamma P - S \tag{2.61}$$

$$\frac{dp}{dt} = \alpha(P_\infty - P) \tag{2.62}$$

$$\frac{dR}{dt} = \beta(X - R) \tag{2.63}$$

As well as the glucose subsystem, the insulin subsystem has a set of metabolic rates, which are described as follows:

$$r_{LIC} = 0.4\left[Q_A^I I_H + Q_G^I I_G + r_{PIR}\right] \tag{2.64}$$

$$r_{KIC} = 0.3 Q_K^I I_K \tag{2.65}$$

$$r_{PIC} = \frac{I_{PF}}{\left(\left((1-0.15)/0.15 Q_P^I\right) - \left(20/V_{PF}^I\right)\right)} \tag{2.66}$$

$$r_{PIR} = \left(\frac{S}{S^B}\right) r_{PIR}^B \tag{2.67}$$

And the inhibitor is modeled with the following equations:

$$S = \begin{cases} [N_1 Y + N_2(X-R)]\,m, \text{ if } X > R \\ N_1 Y m, \text{ if } X \leq R \end{cases} \tag{2.68}$$

$$P_\infty = Y = X^{1.11} \tag{2.69}$$

$$X = \frac{G_H^{3.27}}{132^{3.27} + 5.93 G_H^{3.02}} \tag{2.70}$$

The glucagon subsystem is described with the next equation:

$$\frac{d\Gamma}{dt} = r_{P\Gamma R} - r_{P\Gamma C} \tag{2.71}$$

The metabolic rates for the glucagon subsystem are described below:

$$r_{P\Gamma C} = 9.1\Gamma \tag{2.72}$$

$$r_{P\Gamma R} = M^G_{P\Gamma R} M^I_{P\Gamma R} M^B_{P\Gamma R} \tag{2.73}$$

$$M^G_{P\Gamma R} = 1.31 - 0.61 tanh\left[1.06\left(\frac{G_H}{G_H^B} - 0.47\right)\right] \tag{2.74}$$

$$M^I_{P\Gamma R} = 2.93 - 2.09 tanh\left[4.18\left(\frac{I_H}{I_H^B} - 0.62\right)\right] \tag{2.75}$$

$$r^B_{P\Gamma R} = 9.1 \tag{2.76}$$

And the values for the parameters of the model that were used are described in Table 2.2.

Parameter	Value	Parameter	Value
V_{BV}^{G}	3.5 dl	Q_{G}^{G}	10.1 dl/min
V_{BI}^{G}	4.5 dl	Q_{K}^{G}	10.1 dl/min
V_{H}^{G}	13.8 dl	Q_{P}^{G}	15.1 dl/min
V_{L}^{G}	25.1 dl	Q_{B}^{I}	0.45 l/min
V_{G}^{G}	11.2 dl	Q_{H}^{I}	3.12 l/min
V_{K}^{G}	6.6 dl	Q_{A}^{I}	0.18 l/min
V_{PV}^{G}	10.4 dl	Q_{K}^{I}	0.72 l/min
V_{PI}^{G}	67.4 dl	Q_{P}^{I}	1.05 l/min
V_{B}^{I}	0.26 l	Q_{G}^{I}	0.72 l/min
V_{H}^{I}	0.99 l	Q_{L}^{I}	0.90 l/min
V_{G}^{I}	0.94 l	T_{B}^{G}	2.1 min
V_{L}^{I}	1.14 l	T_{P}^{G}	5 min
V_{K}^{I}	0.51 l	T_{P}^{I}	20 min
V_{PV}^{I}	0.74 l	α	0.0482 min^{-1}
V_{PI}^{I}	0.74 l	β	0.93 min^{-1}
V^{Γ}	99.3 dl	K	0.00794 min^{-1}
Q_{B}^{G}	5.9 dl/min	N_1	0.00747 min^{-1}
Q_{H}^{G}	43.7 dl/min	N_2	0.0958 min^{-1}
Q_{A}^{G}	2.5 dl/min	γ	0.0958 U/min
Q_{L}^{G}	12.6 dl/min	m_0	6.33 U

Table 2.2: Parameters used in the physiological model.

In order to consider meal intake in this model, it was considered a function that describes gastric emptying depending on the amount of carbohydrate intake. It is described in the next subsection.

2.3.1 Gastric emptying model

This model was proposed as part of a physiological model of glucose-insulin interaction of T1DM by Lehmann and Deutsch in 1992 [35]. It considers different rate of gastric emptying depending on the carbohydrate intake, this is if it is greater or equal than 10 CHO gr it is a trapezoidal function but if it is lower than 10 CHO gr it is a triangular function.

$$G_{empt} = \begin{cases} (V_{max}/T_{asc})t, \text{ if } t < T_{asc} \\ V_{max}, \text{ if } T_{asc} < t \leq T_{asc} + T_{max} \\ V_{max} - (V_{max}/T_{des})(t - T_{asc} - T_{max}), \text{ if } T_{asc} + T_{max} \leq t < T_{tot} \\ 0, \text{ elsewhere} \end{cases} \tag{2.77}$$

where G_{empt} (gr CHO/min) is the rate of gastric emptying, V_{max} (gr CHO/min) is the maximal rate of glucose emptying, T_{asc} (min) is the ascending time, T_{max} (min) is the maximal time, T_{des} (min) is the descending time and $T_{tot} = T_{asc} + T_{max} + T_{des}$ (min) is the total time of the function. This carbohydrate intake consideration modifies equation that represents the glucose in the gut, 2.29, where G_{empt} is added. The new equation is stated as follows:

$$\frac{dG_G}{dt} = \left[Q_G^G(G_H - G_G) - r_{GGU+G_{empt}}\right]/V_G^G \tag{2.78}$$

2.4 Parametric adjustment for model personalization

Virtual patient interface is a tool that has rise as an application of mathematical models. In case of diabetes, this tool aims to simulate an specific patient metabolism in order to provide a better vision of a person's actual metabolism [14]. Since mathematical models do not represent an specific patient, they need to be adapted with data of a population of interest. To achieve this a parametric adjustment is needed.

In this research an evolutionary algorithm was used to adapt the model to the gathered data in the experimental study that was performed. More specifically, a modified Evonorm algorithm was implemented. This algorithm originally takes a randomly created group of population (parameters to be tested) to compute the model (evaluation), the result of this calculation is compared to the reference data so that the error can be calculated. After that, the best set of parameters are chosen and then a new population group is created to start a new iteration [36].

The parameters for the implementation of the Evonorm are the total of individuals I, the total of selected individuals Is and total of performed generations TG, where Is has to be less than the 25% of I to have a good performance. The error was calculated as a subtraction of the experimental data and the simulated data. Also, the simulation was done by windows of data, this is that another external iteration was perform to simulate the data point by point. This was done in order to have a better approximation of the simulated data and because of the accumulated energy of the model.

The pseudocode of the classical Evonorm algorithm is as follows [37]:

1.- Uniform random generation of population P of size m.

2.- Evaluation of the total of individuals m.

3.- Selection of the best n individuals ($n < m$).

4.- Calculation of mean and standard deviation from n selected individuals.

5.- Modify standard deviation if intensive exploration is active.

6.- Generation of a new population of size m from random variables with parameters calculated in 4 and 5.

7.- If a criterion is satisfied then end, else go to step 2.

Chapter 3

Analysis of the closed-loop therapy

The aim of this work is to analyze the viability of the closed loop therapy in T2DM. This implies the design of a feedback control system based in a mathematical model able to reproduce the carbohydrate-insulin-glucose dynamics of a T2DM patient. With this idea in mind, the following analyzes were made to the selected mathematical models, in order to choose the most feasible for designing feedback controllers. Regarding the meal simulation model of the glucose-insulin systems, an scheme of parameter and state estimation must be development in order to reproduce the effect of CHO intake in the model. Such effect is defined by the process of rate of glucose appearance Ra, which depends of parameter f, an uncertain parameter in such model. After that a sensitivity analysis of the same model is carried out in order to select a set of parameters to proposed the personalization on the model based on continuous glucose monitoring data.

3.1 Analyzing models for feedback control

Properties of both models were required in order to perform an analysis that allowed a better understanding of the model. With this, they could be adapted to fulfill the objectives of this research. Among these characteristics were: the estimation of uncertain parameters, the parameters sensitivity and equilibrium points. In the next subsections the methodology used to analyze the models is described.

3.1.1 Parameter and state estimation of the meal - glucose - insulin system

Estimation is a helpful tool in the biomedical field because of the lack of sensors to measure many physiological signals. An example of this is in mathematical modeling, where it is necessary to have enough sensed data to validate the models. Numerous applications of mathematical observers or estimators can be found in many areas in order to overcome the lack of sensors; for example, in medical images [38] and in oncology ([39] and [40]).

Mathematical modeling of glucose metabolism has had a major development in the last decades; including systemic models ([41], [42]), black-box models ([43], [44]), and compartmental models ([7], [33]); but not all models are useful in solving the automation of insulin dosage.

An appropriated model for this end must consider the full-relationship from CHO intake to blood glucose concentration. [34] have contributed to solve this problem, they presented a model of glucose metabolism including meal dynamics; however, it depends on the rate of glucose appearance in the intestine (Ra), which is an unmeasured process. In insulin dosage automation, the only available measured variable is glucose concentration; therefore, the model proposed by [34] must be improved in order to provide the full-relationship from CHO intake to blood glucose concentration. For this reason, in this paper we propose an approach to estimate the rate of glucose appearance in the intestine; that is, a sensorless approach to know the effect of CHO intake in glucose metabolism. This idea is sketched in Figure 3.1, we consider the gastric emptying model ([45]) which input is the CHO intake ($D\delta(t)$) and it computes the rate of glucose appearance in the intestine (Ra). In turn, Ra and $D\delta(t)$ are the inputs of the proposed adaptive observer, which is an state affine scheme with exponential convergence to estimate states and uncertain constant parameters. In this case, the observer estimates uncertain parameter f and the state related to mass of glucose in the intestine (Q_{gut}), both from the gastric emptying model. Once the parameter and the state are estimated, the effect of CHO intake can be included in the glucose-insulin metabolism model, which output is the measured blood glucose concen-

tration ($G(t)$).

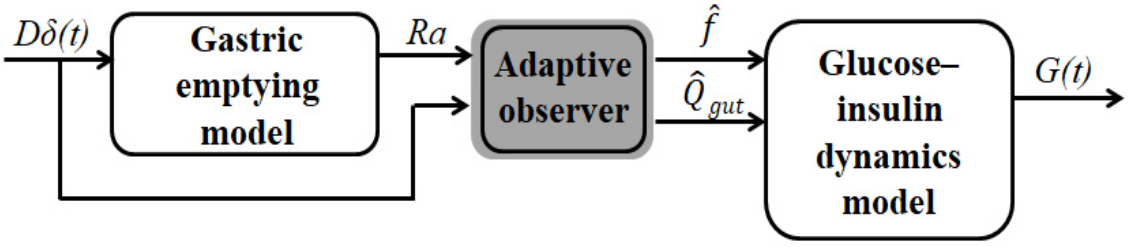

Figure 3.1: Block diagram of the approach to include the effect of CHO intake in glucose-insulin metabolism models. An adaptive observer with exponential convergence is proposed to estimate the rate of glucose appearance in the intestine.

The gastric emptying submodel presented in subsection 2.3.1 is used to model the rate of glucose appearance Ra, which is described in Equation 4.7. The disadvantage of this function is that parameter f is uncertain. Therefore the gastric emptying submodel was disconnected from the glucose-insulin model and by using the adaptive observer proposed by [46], which was used in a cascade system of anaerobic digestion for wastewater, the parameter f and the three states of the submodel were estimated.
For estimation purposes, the process model must be structured as the following state affine system:

$$\begin{cases} \dot{x} = A(y,u)\,x + \beta(y,u) + \varphi(y,u)\,\theta + Bg(y,u,x,\theta) \\ y = Cx \end{cases} \tag{3.1}$$

where $x \in \mathfrak{Re}^n$ is the state vector, $\theta \in \mathfrak{Re}^q$ is the unknown constant parameter vector, $u \in \mathfrak{Re}^l$ is the input vector, $y \in \mathfrak{Re}^r$ is the measurable output. $A(y,u)$, $\beta(y,u)$, $\varphi(y,u)$, $g(y,u,x,\theta)$, B and C are matrices of appropriate dimensions. Furthermore, n, q, l and r are the state space, parameter space, control space, and output space dimensions of system (3.1), respectively.

Considering that $A(y,u)$, $\beta(y,u)$, $\varphi(y,u)$ and $g(y,u,x,\theta)$ satisfy the Assumptions A1-A3 from [46], an adaptive observer for (3.1) is given by:

$$\left\{\begin{array}{rcl} \dot{\hat{x}} & = & A(y,u)\hat{x} + \beta(y,u) + \varphi(y,u)\hat{\theta} + Bg(y,u,\hat{x},\hat{\theta}) \\ & & +\{S_L^{-1}C^T + \Lambda\Gamma^{-1}\Lambda^T C^T\}Q(y - C\hat{x}) \\ \dot{S}_L & = & -\rho S_L - A^T(y,u)S_L - S_L A(y,u) + C^T QC \\ \dot{\Lambda} & = & \{A(y,u) - S_L^{-1}C^T QC\}\Lambda + \varphi(y,u) \\ \dot{\Gamma} & = & -\lambda\Gamma + \Lambda^T C^T QC\Lambda \\ \dot{\hat{\theta}} & = & \Gamma^{-1}\Lambda^T C^T Q(y - C\hat{x}) \end{array}\right. \tag{3.2}$$

where $\hat{x}$ and $\hat{\theta}$ are estimations of x and θ, respectively. The parameters $\rho \in \mathfrak{Re}$ and $\lambda \in \mathfrak{Re}$ modify the gains $S_L \in \mathfrak{Re}^{n\times n}$, $\Lambda \in \mathfrak{Re}^{n\times q}$ and $\Gamma \in \mathfrak{Re}^{q\times q}$, of the observer for n states, l inputs, r outputs and q unknown parameters. $Q \in \mathfrak{Re}^{r\times r}$, S_L and Γ are positive definite symmetric matrices. The exponential convergence proof of the adaptive observer (3.2) to system (3.1) is demonstrated in [46]. By means of some algebraic manipulation, the system (2.23)-(2.25) and (4.7) can be written as (3.1) with:

$$x = \begin{bmatrix} x_1 \\ x_2 \\ x_3 \end{bmatrix} = f \begin{bmatrix} Q_{sto1}(t) \\ Q_{sto2}(t) \\ Q_{gut}(t) \end{bmatrix} \tag{3.3}$$

$$\theta = f, \quad u = D\delta(t), \quad y = Ra(t),$$

$$A(y,u) = \begin{bmatrix} -k_{gri} & 0 & 0 \\ k_{gri} & -k_{max} & 0 \\ 0 & k_{max} & -k_{abs} \end{bmatrix},$$

$$\beta(y,u) = \begin{bmatrix} 0 \\ 0 \\ 0 \end{bmatrix}, \quad \varphi(y,u) = \begin{bmatrix} D\delta(t) \\ 0 \\ 0 \end{bmatrix},$$

$$B = \begin{bmatrix} 0 \\ -\frac{(k_{max}-k_{min})}{2} \\ \frac{(k_{max}-k_{min})}{2} \end{bmatrix},$$

$$g(y,u,x,\theta) = [\tanh(w) - \tanh(v)]\, x_2,$$

$$w = \frac{5(x_1+x_2)}{2Df(1-b)} - \frac{5b}{2(1-b)},$$

$$v = \frac{5(x_1+x_2)}{2Dcf} - \frac{5}{2},$$

$$\text{and} \quad C = \begin{bmatrix} 0 & 0 & \frac{k_{abs}}{BW} \end{bmatrix}.$$

Then, the adaptive observer (3.2) and the scalar mapping (3.3) allow the estimation of $\hat{Q}_{sto1}(t)$, $\hat{Q}_{sto2}(t)$, $\hat{Q}_{gut}(t)$ and $\hat{f}$ of the states $Q_{sto1}(t)$, $Q_{sto2}(t)$, $Q_{gut}(t)$ and parameter f, respectively; if the next assumptions hold:

(i) The system (2.23)-(2.25) is completely observable.

(ii) The Assumptions A1-A3 from [46] are satisfied.

Then, the estimation of $Ra(t)$ is computed as:

$$\hat{Ra}(t) = \frac{k_{abs}\hat{x}_3}{BW}. \tag{3.4}$$

3.1.2 Sensitivity analysis

Since one of the objectives is to describe the glucose-insulin dynamics of a T2DM patient, it is necessary to do a parametric adjustment. Before that adjustment can be done, it is important to know the change of the states of the model respect

of each parameter. For this purpose, a sensitivity analysis with nominal values was proposed for the meal simulation model. For this analysis, the model was written in its state-space form such that $x_1 = G_p$, $x_2 = G_t$, $x_3 = I_l$, $x_4 = I_p$, $x_6 = I_d$, $x_7 = Q_{sto1}$, $x_8 = Q_{sto2}$, $x_9 = Q_{gut}$, $x_{10} = X$, $x_{11} = I_{po}$ and $x_{12} = Y$. The sensitivity equation used to make this analysis is proposed in [47] as follows:

$$\dot{S}(t) = A(t,P)S(t) + B(t,P) \tag{3.5}$$

where:

$$A(t,P) = \frac{\partial f(x,P)}{\partial x}\,|_{P_0} \tag{3.6}$$

$$B(t,P) = \frac{\partial f(x,P)}{\partial P}\,|_{P_0} \tag{3.7}$$

where x are the states of the model, P are the total of the parameters, P_0 are the nominal values of the parameters, A is the matrix of the partial derivative of the model equations with respect of the states of size $(n \times n)$, where n represents the total number of states; B is the matrix of the partial derivative of the model equations with respect of the parameters of size $(n \times m)$, where m represents the total number of parameters, and finally, $S(t)$ represents the sensitivity function $(n \times m)$.

3.1.3 Equilibrium points and model linearization

In order to analyze the dynamics of the model in equilibrium, it is necessary to know at which value each equation rests, for this purpose, equilibrium points come in hand. An equilibrium point x^* satisfies the expression $\frac{dx}{dt} = 0 \Leftrightarrow x = x^*$, where the value of x^* is a constant. The physiological model for T2DM was written in its state-space form to get the equilibrium points and the system linearization. Perturbations were not considered in the linearization.

$$\dot{x_1} = -2.2979x_1 + 0.6122x_2 + 1.6857x_3 \tag{3.8}$$

$$\dot{x_2} = 0.4761x_1 - 0.4761x_2 - 15.5555 \tag{3.9}$$

$$\dot{x_3} = 0.4275x_1 - 3.1666x_3 + 0.9130x_5 + 0.7318x_6 + 1.0942x_7 - 0.7246 \tag{3.10}$$

$$\dot{x_4} = 0.9017x_3 - 0.9017x_4 - 1.7857 \tag{3.11}$$

$$\begin{aligned}\dot{x_5} &= 0.0996x_3 + 0.4023x_4 - 0.5019x_5 - 0.7968x_{22}[2.232tanh(0.0146x_5) \\ &- 2.4836 + 2.201] + 6.1752x_{20}[1.406tanh(0.0048x_5) - 0.3081 \\ &- 1.425][x_{21}tanh(0.39x_{19})]\end{aligned} \tag{3.12}$$

$$\dot{x_6} = 1.5303x_3 - 1.5304x_6 - 10.7575tanh(0.011x_6) - 5.06 - 10.7575 \tag{3.13}$$

$$\dot{x_7} = 1.4519x_3 - 2.6634x_7 + 1.2115x_8 \tag{3.14}$$

$$\dot{x_8} = 0.2x_7 - 0.2x_8 - 0.0048x_8(1.915tanh(0.3340x_{15}) - 2.3020 + 2.788) \tag{3.15}$$

$$\dot{x_9} = -1.6981x_9 + 1.6981x_{10} \tag{3.16}$$

$$\dot{x_{10}} = 0.4568x_9 - 3.1675x_{10} + 0.9137x_{12} + 0.7309x_{13} + 1.0659x_{14} \tag{3.17}$$

$$\dot{x_{11}} = 0.7619x_{10} - 0.7619x_{11} \tag{3.18}$$

$$\begin{aligned}\dot{x_{12}} &= 0.0947x_{10} + 0.3789x_{11} - 0.7894x_{12} + 0.7412x_{18}\left(\frac{x_3^{\frac{327}{100}}}{5.93x_3^{\frac{151}{50}}}\right) \\ &+ 8595611.0407^{\frac{111}{100}}\end{aligned} \tag{3.19}$$

$$\dot{x_{13}} = 0.9980x_{10} - 1.4257x_{13} \tag{3.20}$$

$$\dot{x_{14}} = 1.4285x_{10} - 1.8870x_{14} + 0.4585x_{15} \tag{3.21}$$

$$\dot{x_{15}} = 0.05x_{14} - 0.1167x_{15} + 0.1483I \tag{3.22}$$

$$\dot{x_{16}} = \frac{0.0482x_3^{\frac{327}{100}}}{5.93x_3^{\frac{151}{50}}} + 8595611.04^{\frac{111}{100}} - 0.0482x_{16} \tag{3.23}$$

$$\dot{x_{17}} = \frac{0.931x_3^{\frac{327}{100}}}{5.93x_3^{\frac{151}{50}}} + 8595611.04077 - 0.931x_{17} \tag{3.24}$$

$$\begin{aligned}\dot{x_{18}} &= 0.575x_{16} - 0.00794x_{18} - 0.00595x_{18}\left(\frac{x_3^{\frac{37}{100}}}{5.93x_3^{\frac{151}{50}}}\right) + 8595611.04^{\frac{111}{100}} \\ &+ 0.0505 \end{aligned} \tag{3.25}$$

$$\begin{aligned}\dot{x_{19}} &= 0.0916[2.09tanh(0.035x_3 - 2.5916)] \\ &- 2.93[0.61tanh(0.2002x_{10} - 0.4982) - 1.31] - 0.0916 \end{aligned} \tag{3.26}$$

$$\dot{x_{20}} = 0.02764 - 0.025tanh(0.1332x_{12}) - 1.5369 - 0.04x_{20} \tag{3.27}$$

$$\dot{x_{21}} = 0.0207tanh(0.39x_{19}) - 0.015x_{21} - 0.0076 \tag{3.28}$$

$$\dot{x_{22}} = 0.0249tanh(0.1193x_{12}) - 0.63921 - 0.04x_{22} + 0.0338 \tag{3.29}$$

By making these equations equal to zero, the obtained equilibrium points are:

$$x^* = [128.6764\ \ 96.0097\ \ 140.5408\ \ 138.5606\ \ 149.990\ \ 140.5408\ \ 137.9540$$
$$135.0563\ \ 8.7353\ \ 8.7353\ \ 8.7353\ \ 11.8766\ \ 6.7194\ \ 7.4250\ \ 3.3424\ \ 1.1634$$
$$0.7559\ \ 0.5568\ \ 2.6994\ \ 8.3868\ \ 0.3558\ \ 0.3941].$$

After the equilibrium points have been found, the jacobian matrices have to be calculated in order to get the model linearization, this is done by rewriting the model in the form presented in 3.30.

$$\begin{cases} \dot{x} = Ax + Bu \\ y = Cx \end{cases} \tag{3.30}$$

where matrices $A = \frac{\partial f}{\partial x}\ |_{x^*}$, $B = \frac{\partial f}{\partial u}\ |_{x^*}$, and C is the output signal of the model; where f are the functions, x are the states and u is the control input signal. After performing the partial derivatives and the evaluation around the equilibrium point, the stated matrices are presented in section 4.5. Also, in this section, the

results of the performance of the control are stated. This scheme was proved with different CHO intakes in six days.

3.2 Closed-loop controllers in T2DM

One of the main objectives of working with diabetes mellitus models is to have a control scheme that aims to the blood glucose level regulation. Most of the work done in reference of this control objective is for T1DM. Nevertheless, there are many researches that have proved that insulin therapy for T2DM is an effective methodology to lower glucose levels ([48], [49], [50]). In controllers for T2DM, the most outstanding researches use tools as classic control or intelligent algorithms. An example of the first one is the scheme proposed by Sun *et al.*, where he used a proportional-integral-derivative (PID) controller to maintain normoglycemic levels for T2DM patients, considering a closed-loop insulin infusion pump, short-acting insulin absorption and gut absorption [51]. Their preliminary results show the potential use of control algorithms for regulation. Also, by fusing classical control and intelligent algorithms, Ekram *et al.* proposed the usage of a proportional-integral (PI) controller with a modification by penalising the feedback error using a fuzzy inference system [52]. They reported that the fuzzy-based PI controller had a better performance than the conventional PI controller in glucose regulation.

In this research, a classic PID controller is proposed in order to have a preliminary analysis of the viability of the closed-loop therapy for T2DM. This controller is the most common control algorithm used in industry due to the robust performance and functional simplicity [53]. This controller have a feedback control signal that depends in the error signal. The control signal is calculated by considering three characteristics to process the controlled output signal: to cancel the error in the actual instant, to measure the amount of time that the signal has kept the wrong values and to anticipate the future errors by measuring the variation rate at each instant [54]. The equation for the control law is given by equation 3.31.

$$u(t) = K_p e(t) + K_i \int_0^t e(t)dt + K_d \frac{d}{dt} e(t) \tag{3.31}$$

The problem that is wanted to solve with the application of a PID controller is that the system get to the normoglycemic range, between 70 mg/dl and 120 mg/dl, that is a regulation problem rather than a tracking problem. The main idea is to have an insulin signal that depends on time to adjust the dose with respect of the blood glucose level response, in order to maintain the metabolism in a desired glucose level.

The general closed-loop scheme is represented in Figure 3.2, where the gut absorption of the CHO intake is the perturbation to the system and the insulin ($u(t)$) is the control signal that goes into the glucose-insulin dynamic model (in this case the physiological model for T2DM was used), as can be seen in the next equation, where $u(t)$ is added to the original differential equation of I_{PI} (Eq. 2.60):

$$\frac{dI_{PI}}{dt} = \left[\frac{V_{PI}^I}{T_P^I}(I_{PV} - I_{PI}) - r_{PIC} + u(t) \right] / V_{PI}^I$$

A reference value is given considering the normoglycemic range and the feedback signal is the blood glucose level.

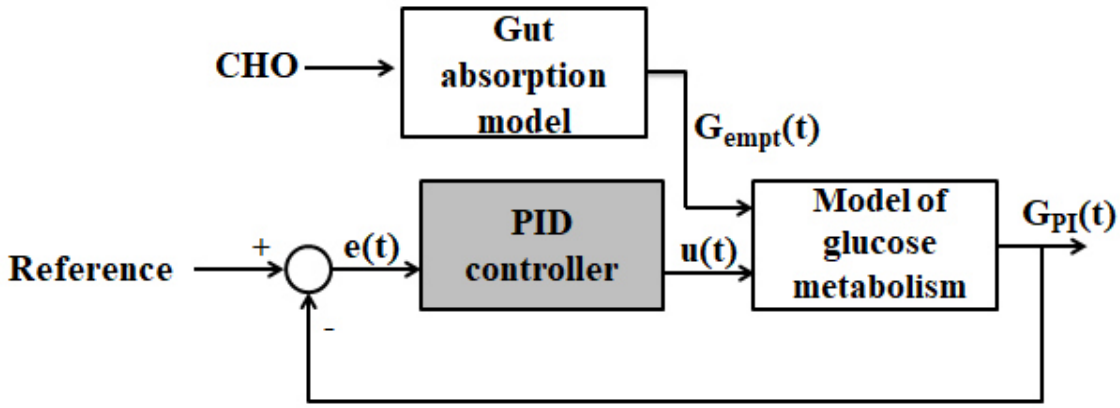

Figure 3.2: General control scheme to analyze the viability of the insulinization therapy, where the reference is a stated value of the normoglycemic range (between 70 mg/dl and 120 mg/dl), $G_{PI}(t)$ is the peripheral interstitial glucose concentration, $e(t)$ is the error between the reference signal and $G_{PI}(t)$, $u(t)$ is the control signal gathered from the PID controller, CHO is the amount of carbohydrate intake, and $G_{empt}(t)$ is the rate of gastric emptying.

Chapter 4

Results

In this section the results of this research are reported. It is structured as follows: first, the experimental set up to obtain continuous glucose monitoring data of T2DM patients is presented. After that, results of the scheme to estimate the parameter f and the sensitivity analysis of the meal simulation model are presented. Then, results of the parametric adjustment scheme for the physiological model are presented. Finally, the closed-loop control scheme is proved in the physiological model, the results are also presented here.

4.1 Experimental set up

Along with Hospital Universitario "Dr. José Eleuterio González" a prospective and longitudinal cohort study was performed in order to characterized the dynamic behaviour of the glucose metabolism in T2DM patients. The study considered 20 patients who fulfilled the features described in Table 4.1. The study was complete in 90 days, in this time the patients recorded their meal intake, postprandial glucose concentration (two hours after meal intake) and insulin and metformin supply. Also a continuous glucose monitor (CGM) was carried by the patients during a week, this permitted to get a report of their blood glucose concentrations every five minutes.

Age range	Between 30 and 70 years old
Time from diagnosis	2 years
Current treatment	At least two oral medicines
Body mass index (BMI)	Between 26 and 40 kg/m^2
% Hb1Ac	Between 7.5% and 10%
Fasting glucose concentration	≥140 mg/dl

Table 4.1: Criteria for acceptance of T2DM patients into the experimental study.

In order to perform the parametric adjustment, data from a patient was used. In Table 4.2 and in Table 4.3, respectively, CHO intake and postprandial glucose concentrations are reported. In Figure 4.1 the glucose concentration curves of each day is presented.

	Breakfast	**Lunch**	**Dinner**
	MI (gr CHO)	MI (gr CHO)	MI (gr CHO)
Day 1	45.95	73	60
Day 2	45.95	22.5	82.5
Day 3	45.95	23.4	22.5
Day 4	45.95	5	15
Day 5	45.95	15	49.4
Day 6	45.95	36.3	49.4

Table 4.2: Patient data. Meal intake (MI) measured in grams of CHO.

	Breakfast	**Lunch**	**Dinner**
	GC (mg/dl)	GC (mg/dl)	GC (mg/dl)
Day 1	117	195	174
Day 2	153	215	143
Day 3	192	187	168
Day 4	160	134	188
Day 5	104	191	189
Day 6	131	225	178

Table 4.3: Patient data. GC (glucose concentration) measured in mg/dl, it was taken two hours after meal intake (postprandial).

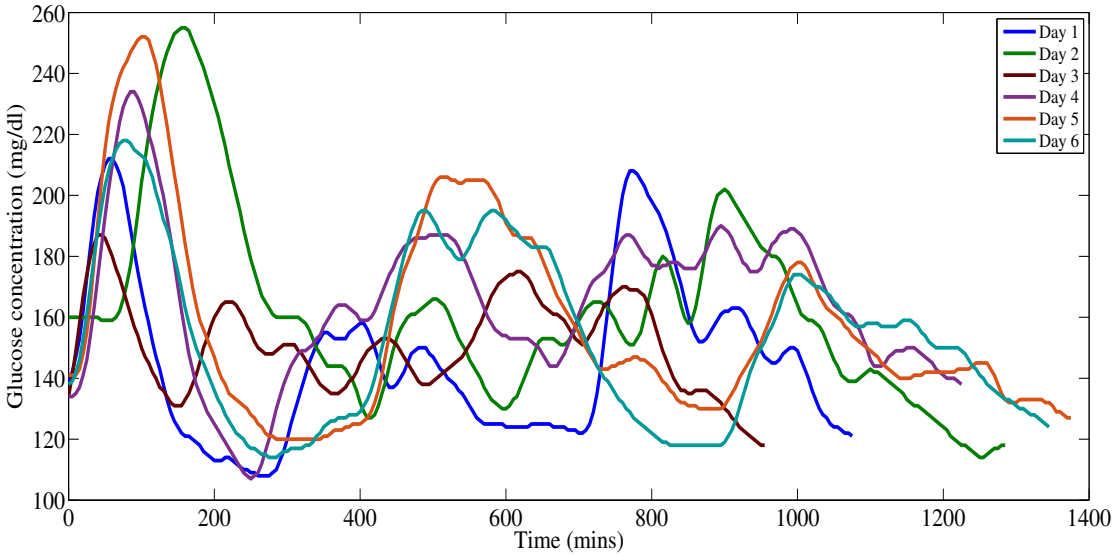

Figure 4.1: Glucose concentration curves of six days of continuous glucose monitoring every five minutes.

4.2 Parameter and state estimation

The proposed scheme is given by equations of the meal-glucose-insulin model given by equations (2.23)-(2.25), and the adaptive observer defined in (3.2). The numerical implementation of the whole system was coded in MATLAB® using the differential equation solver *ode45*. The simulation time was $t \in [0, 4000]$ minutes, and the vector of initial conditions for the model was $x_0 = [0\ 0\ 0]^T$. Since the CHO intake is made in fasting conditions, this is when the stomach is empty, the initial conditions for the gastric emptying model were stated in zero.

To obtain acceptable results three meals were considered in the numerical implementation, as described in Figure 4.2. Each meal was considered as the perturbation performed by $D\delta(t)$, and it was modeled as a train of five square pulses, with period of 6 minutes, giving a total of 30 minutes of CHO intake (see Figure 4.2).

In order to illustrate the convergence of the estimated states, three different sets of initial conditions were arbitrarily stated as $\hat{x}_1(0) = \hat{x}_2(0) = \hat{x}_3(0) = 3\text{x}10^5$, $\hat{x}_1(0) =$

$\hat{x}_2(0) = \hat{x}_3(0) = 4\text{x}10^5$ and $\hat{x}_1(0) = \hat{x}_2(0) = \hat{x}_3(0) = 9\text{x}10^5$ considering the initial condition for the estimated parameter as $\hat{f}(0) = 0.5$, $S_L(0) = [I] \in \Re\mathfrak{e}^{3\times3}$, $\Lambda(0) = \Gamma(0) = 1$. The nominal values of parameter of the model (2.23)-(2.25) are reported in Table 4.4, as well as the gains of the adaptive observer. The estimation of states can be verified in Figure 4.4 - 4.5.

Moreover, the convergence of the estimated parameter $\hat{f}$ is shown in Figure 4.6, considering three different initial conditions chosen as $\hat{f}(0) = 0.25$, $\hat{f}(0) = 0.5$ and $\hat{f}(0) = 3$. The resulting estimation of Ra is shown in Figure 4.7. The gastric emptying submodel is reconnected to the glucose metabolism model proposed by Dalla Man *et al.*, the glucose concentration can also be obtained, this is shown in Figure 4.8. In all these figures, the original (solid line) and estimated (dash line) value are presented.

Parameter	**Value**
k_{gri}	$0.0558\ min^{-1}$
k_{max}	$0.0558\ min^{-1}$
k_{min}	$0.008\ min^{-1}$
k_{abs}	$0.057\ min^{-1}$
D	$78000\ mg$
b	0.82
c	$0.00236\ mg^{-1}$
BW	$78\ kg$
f	1.2723
ρ	0.0710
λ	2

Table 4.4: Nominal values for the parameter of the model and adaptive observer proposed by [34].

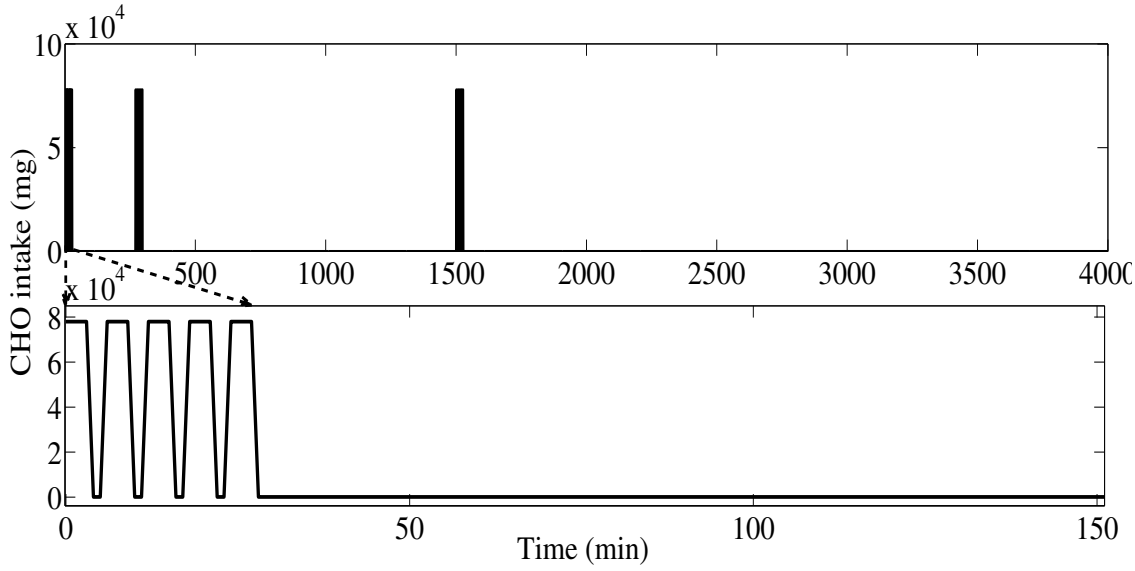

Figure 4.2: CHO intake is modeled by $D\delta(t)$ as a train of five square pulses, with period of 6 minutes, giving a total of 30 minutes per meal. The disturbance is presented in the full simulation time (top), and a zoom in of a single meal is also included (bottom).

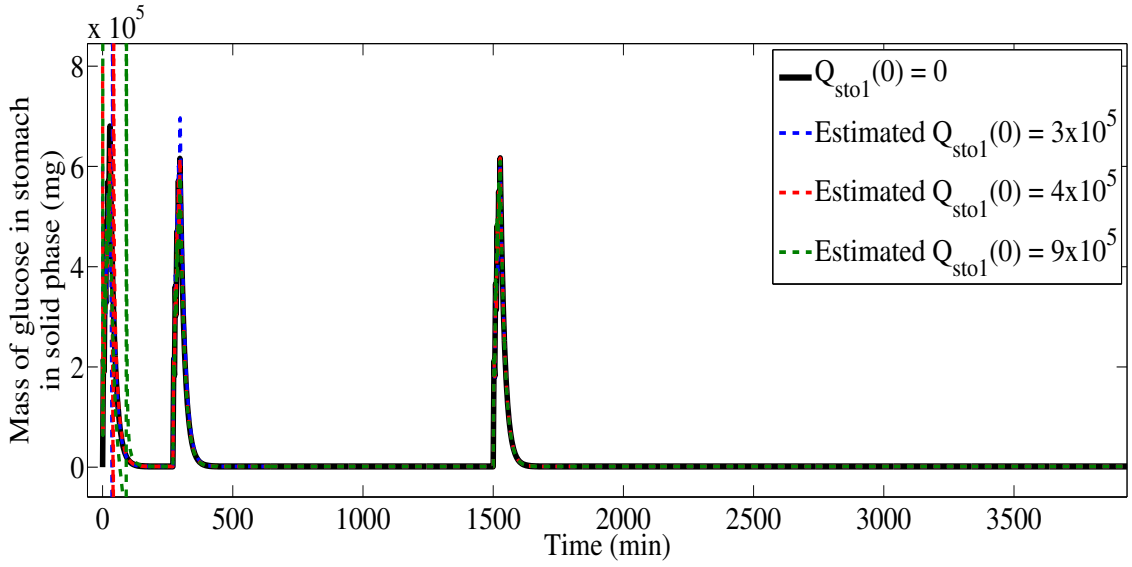

Figure 4.3: Estimation of the glucose mass in solid phase, Q_{sto1}.

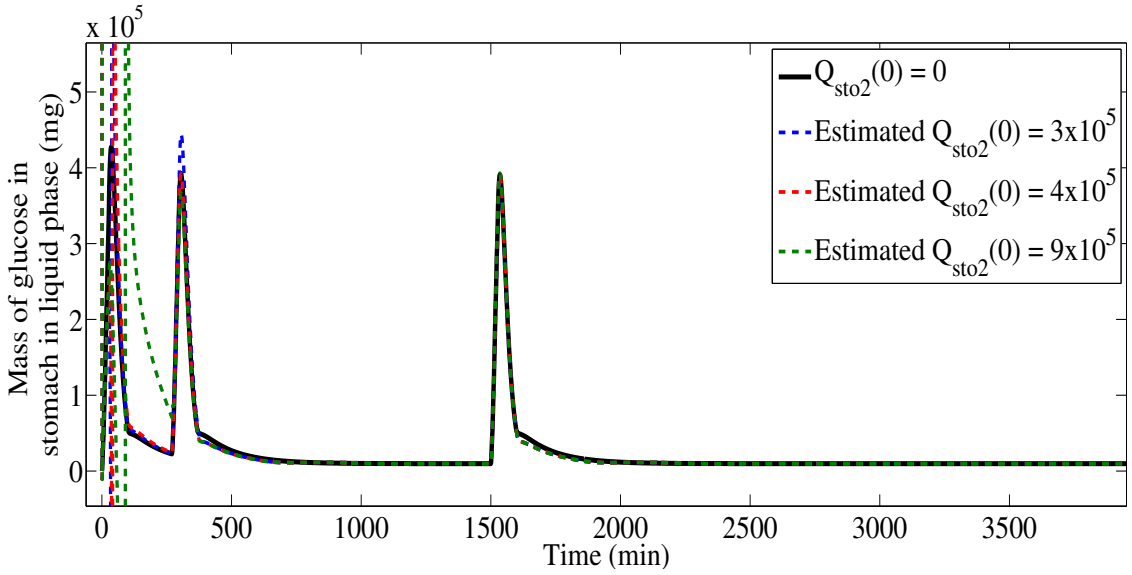

Figure 4.4: Estimation of the glucose mass in liquid phase, Q_{sto2}.

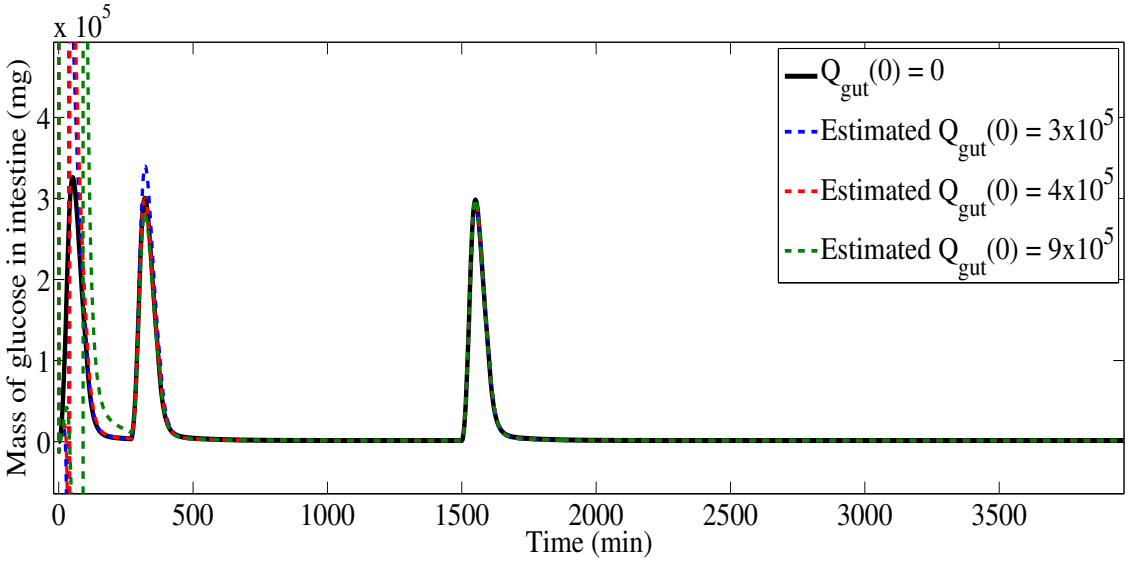

Figure 4.5: Estimation of the glucose mass in the intestine, Q_{gut}.

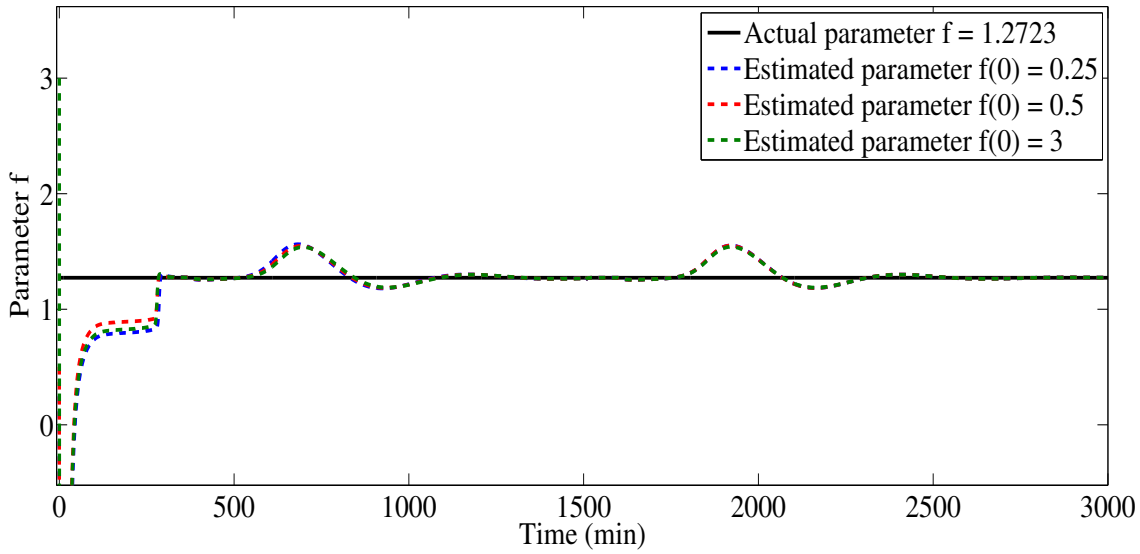

Figure 4.6: Estimation of the uncertain parameter f involved in modeling of rate of glucose rate appearance, Ra.

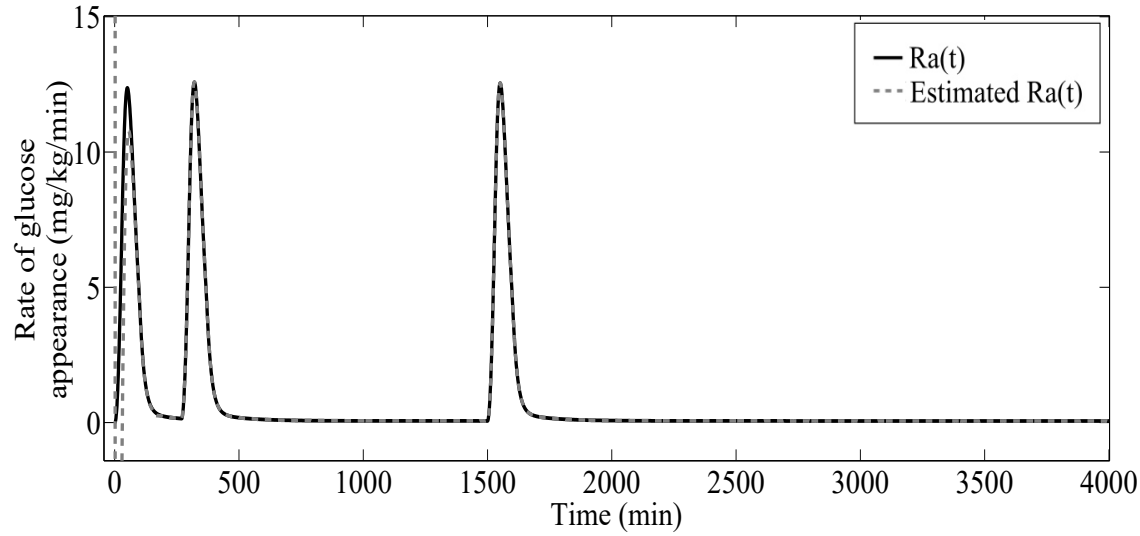

Figure 4.7: Estimated vs original value of rate of glucose rate appearance, Ra.

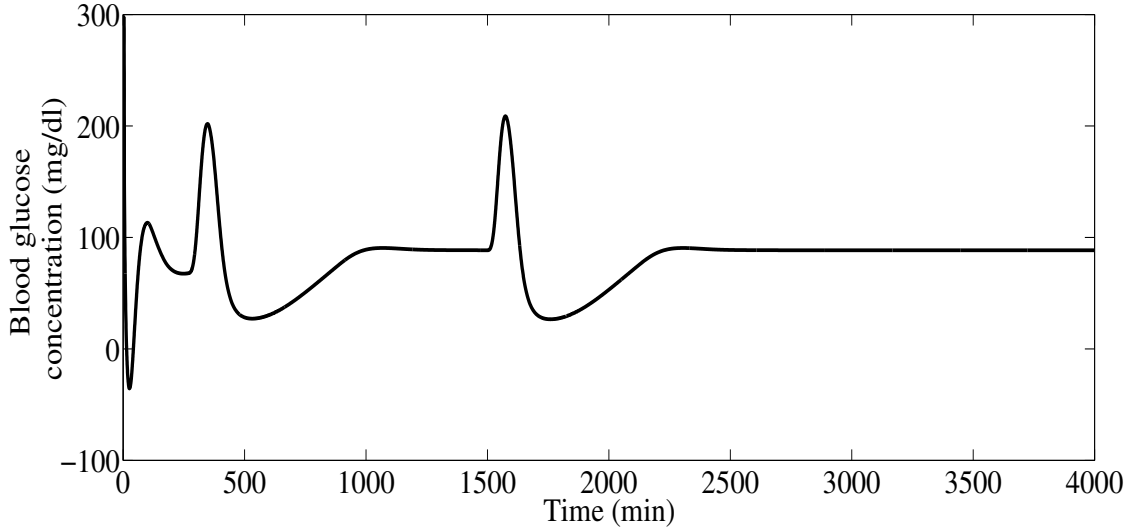

Figure 4.8: Effect of the estimated disturbance in the glucose-insulin metabolism model by CHO intake.

4.3 Sensitivity analysis

As said in Section 3.1.2, the sensitivity analysis of the meal-glucose-insulin model was performed by implementing Equation 3.5. Considering that the total number of states n was 12, and the total number of parameters m was 37, the dimension of the matrices were $A(t,P)$ of 12×12, $S(t)$ of 12×37, and $B(t,P)$ of 12×37. The parameters that were considered for this analysis were: k_{p1}, k_{p2}, k_{p3}, k_{p4}, f, k_{abs}, BW, F_{cns}, k_{e1}, k_{e2}, k_1, k_2, V_{m0}, V_{mx}, K_{m0}, m_1, m_2, m_4, m_5, m_6, γ, k_i, V_I, k_{max}, k_{min}, b, c, k_{gri}, p_{2u}, I_b, K, S_b, α, β, h, V_G and D.

The range of consideration for a parameter to be sensible was $\pm$ 400. With this in mind, the most sensible parameters were: k_{p2}, k_{p3}, k_1, k_2, k_{e1}, V_I, α and β. This parameters affect in Equations 2.1, 2.2, 2.25, as can be seen below. Since the equation of interest was Equation 2.1, which models the mass of glucose in plasma and rapidly equilibrating tissues and is needed in Equation 2.10, in order to model the glucose concentration, the sensitivity analysis results for this equation can be seen in Figure 4.9.

$$
\begin{aligned}
\frac{dG_p(t)}{dt} &= EGP(t) + Ra(t) - U_{ii}(t) - E(t) - k_1 G_p(t) \\
&+ k_2 G_t(t) \\
\frac{dG_t(t)}{dt} &= -U_{id}(t) + k_1 G_p(t) - k_2 G_t(t) \\
EGP(t) &= k_{p1} - k_{p2} G_p(t) - k_{p3} I_d(t) - k_{p4} I_{po}(t) \\
E(t) &= \begin{cases} k_{e1}[G_p(t) - k_{e2}], & \text{if } G_p(t) > k_{e2} \\ 0 & \text{if } G_p(t) \leq k_{e2} \end{cases} \\
I(t) &= \frac{Ip(t)}{V_I} \\
\frac{dY(t)}{dt} &= \begin{cases} -\alpha[Y(t) - \beta(G(t) - h)], & \text{if } \beta(G(t) - h) \geq -S_b \\ -\alpha * Y(t) - \alpha * S_b, & \text{if } \beta(G(t) - h) < -S_b \end{cases}
\end{aligned}
$$

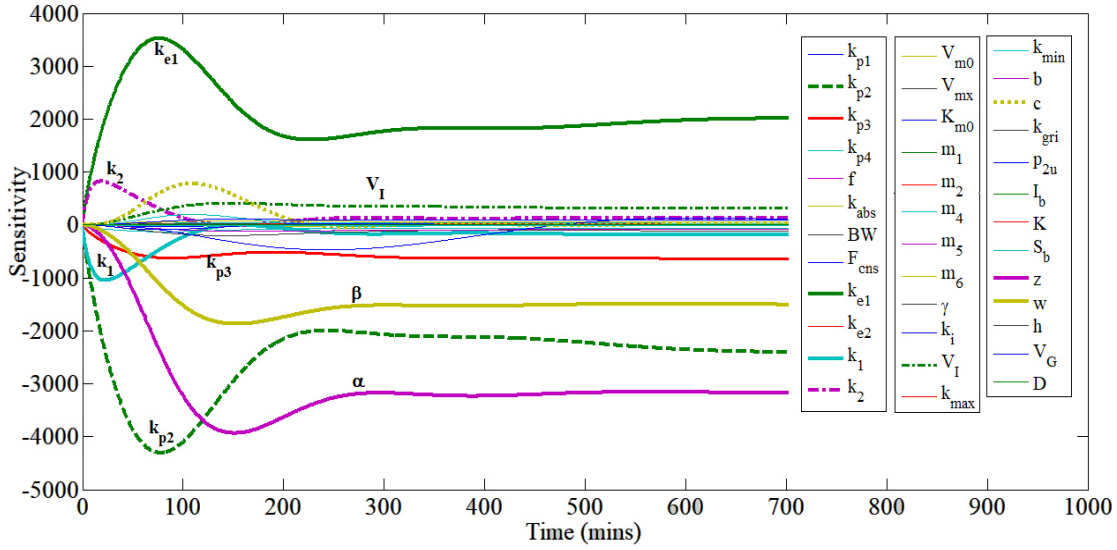

Figure 4.9: Sensitivity analysis results for state x_1, which is described by Equation 2.1. The most sensible parameteres were: k_{p2}, k_{p3}, k_1, k_2, k_{e1}, V_I, α and β. The range of consideration as a sensible parameter is between ± 400.

Back in 2007, a sensitivity analysis for the physiological model for T1DM, proposed by Sorensen in [7], was previously reported by Quiroz and Femat in [55].

It was stated that there were four most sensitive parameters related to metabolic parameters.

4.4 Parametric adjustment

The parametric adjustment was performed for both models. Since the results of the meal-glucose-insulin model were not conclusive, they are not presented. Therefore, the parametric adjustment outcome shown in this section was obtained from the physiological model. Eighteen parameters were chosen from the metabolic rates to perform the adjustment:

$$
\begin{aligned}
M^{I}_{PGU} &= 2.788 + 1.915 tanh\left[0.619\left(\frac{I_{PF}}{I^{B}_{PF}} - 3.719\right)\right] \\
M^{G}_{HGU} &= 2.201 + 2.232 tanh\left[1.883\left(\frac{G_{L}}{G^{B}_{L}} - 1.319\right)\right] \\
M^{I\infty}_{HGU} &= 0.845 + 0.624 tanh\left[0.894\left(\frac{I_{L}}{I^{B}_{L}} - 0.715\right)\right] \\
M^{I\infty}_{HGP} &= 0.691 - 0.626 tanh\left[0.998\left(\frac{I_{L}}{I^{B}_{L}} - 1.54\right)\right] \\
S &= \begin{cases} [N_1 Y + N_2(X - R)]\, m, \text{ if } X > R \\ N_1 Y m, \text{ if } X \leq R \end{cases}
\end{aligned}
\tag{4.1}
$$

Recalling Subsection 2.4, an evolutionary algorithm was used to perform the parametric adjustment. The implementation of the Evonorm algorithm was coded in MATLAB®. According to the physiological model proposed by Vahidi *et al*, they stated that in T2DM 18 parameters related with metabolic rates change regarding healthy condition. Then those 18 parameters were adjusted with the algorithm, the equations that involve these parameters are presented above. The information was separated as three events: breakfast, lunch and dinner, in order to have a more accurate performance of the algorithm and to diminish the simulation time. The parameters used in the implementation of the Evonorm

Day	Breakfast	Lunch	Dinner
1	3.3408	3.4935	*Dismiss*
2	*Dismiss*	*Dismiss*	4.4552
3	5.8690	7.73	11.5011
4	3.33	11.8855	12.6632
5	7.8482	*Dismiss*	26.7860
6	4.7072	9.8081	13.2906

Table 4.5: Mean errors obtained in each simulation for the parametric adjustment. The *Dismiss* legend indicates that the error of the adjustment was either too big or a complex number.

algorithm were total of individuals I, stated as 100 individuals, selected individuals Is, stated as 20 individuals, and total of performed generations TG, stated as 150 generations. About the generation of new individuals, the upper range for the new individuals generation was left opened and the lower range was left as 1×10^{-5} to allow a wider search for the parameters.

The performance of the algorithm with the 18 events can be seen in Table 4.5 along with the mean error of each one. The accepted error was less than 14 mg/dl, that is lower than the average accepted error from glucometers. The results from the simulations are reported in Figures 4.10, 4.11 and 4.12.

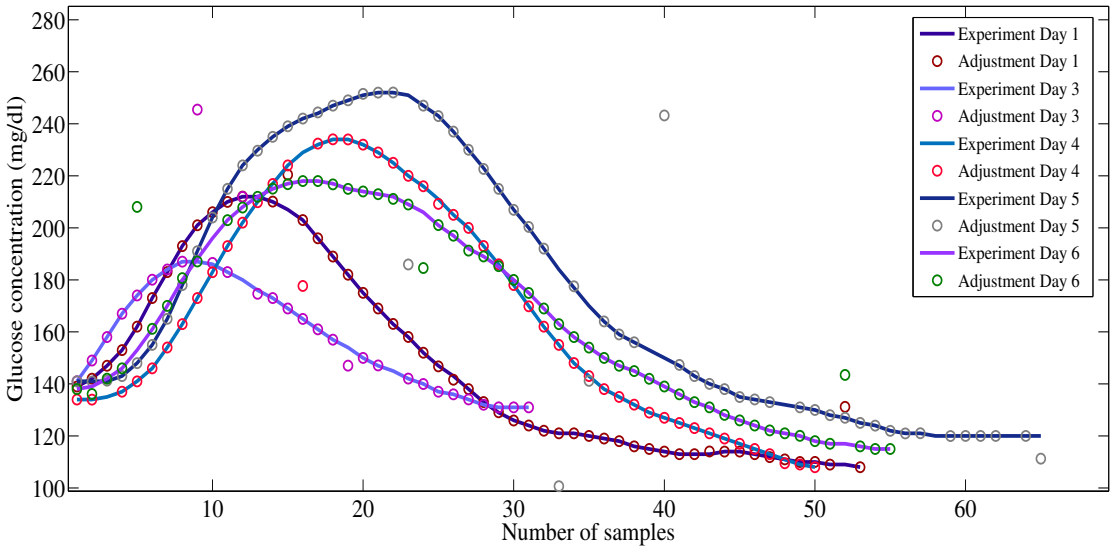

Figure 4.10: Tracking curves of the parametric adjustment of the physiological model of glucose metabolism during breakfast meal.

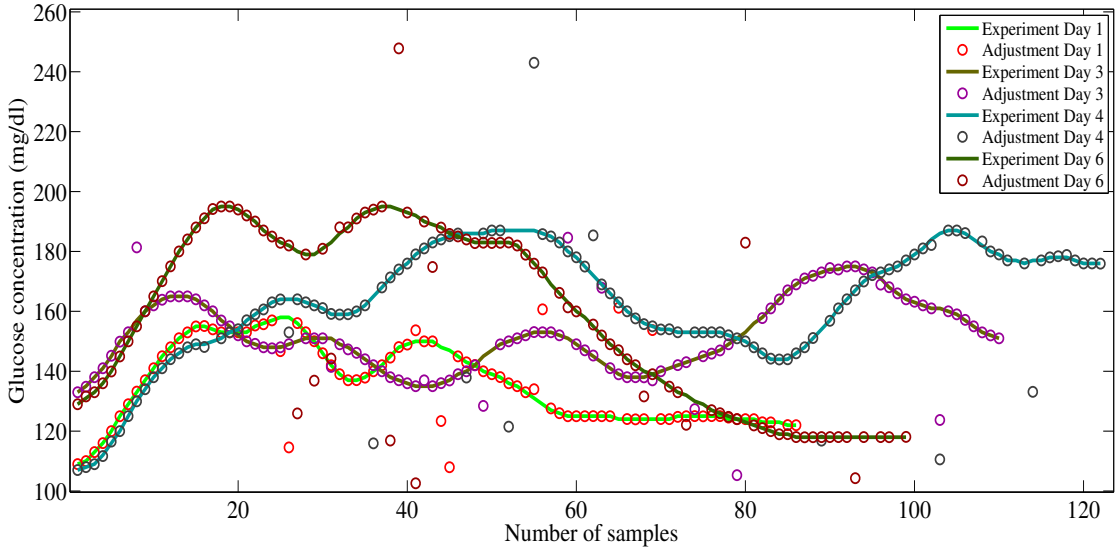

Figure 4.11: Tracking curves of the parametric adjustment of the physiological model of glucose metabolism during dinner meal.

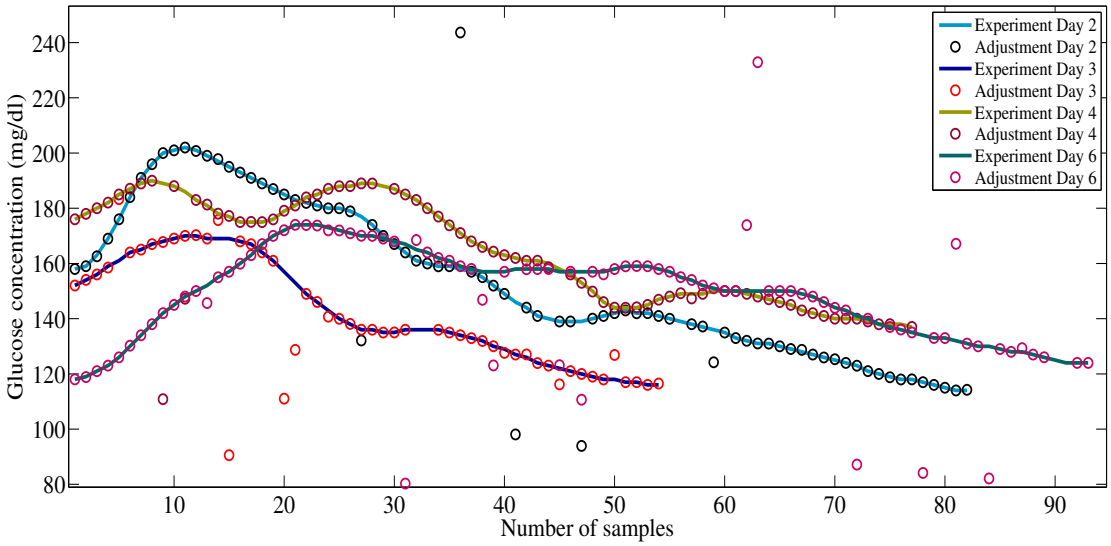

Figure 4.12: Tracking curves of the parametric adjustment of the physiological model of glucose metabolism during breakfast.

The mean absolute error with its standard deviation was considered for each event in order to have a better understanding of the performance of the evolutionary algorithm. The best three simulations were chosen in order to calculate the mean error for each event. This can be seen in Figures 4.13, 4.14 and 4.15.

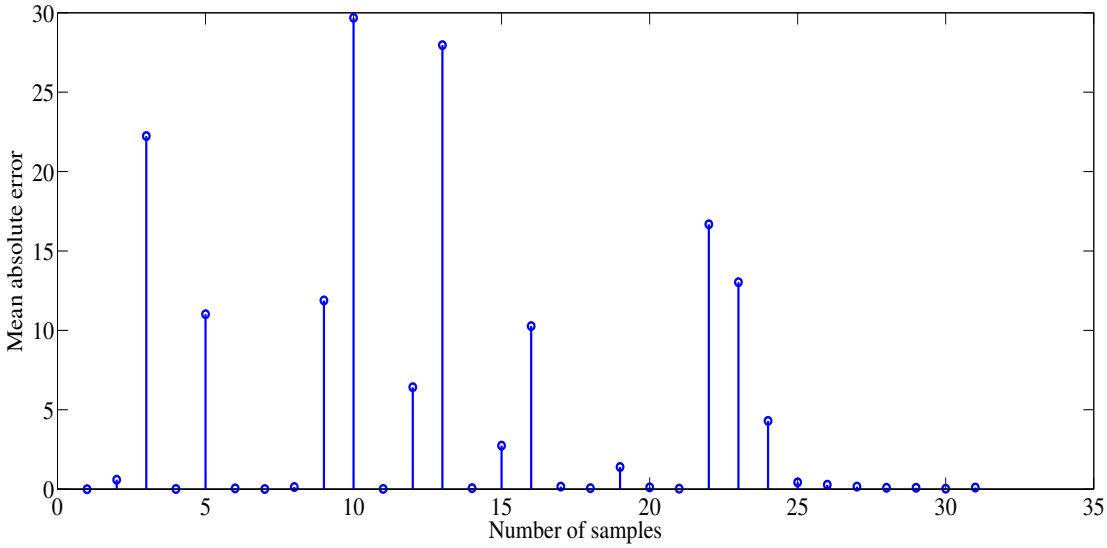

Figure 4.13: Mean absolute error of breakfast event of days 1, 4 and 6.

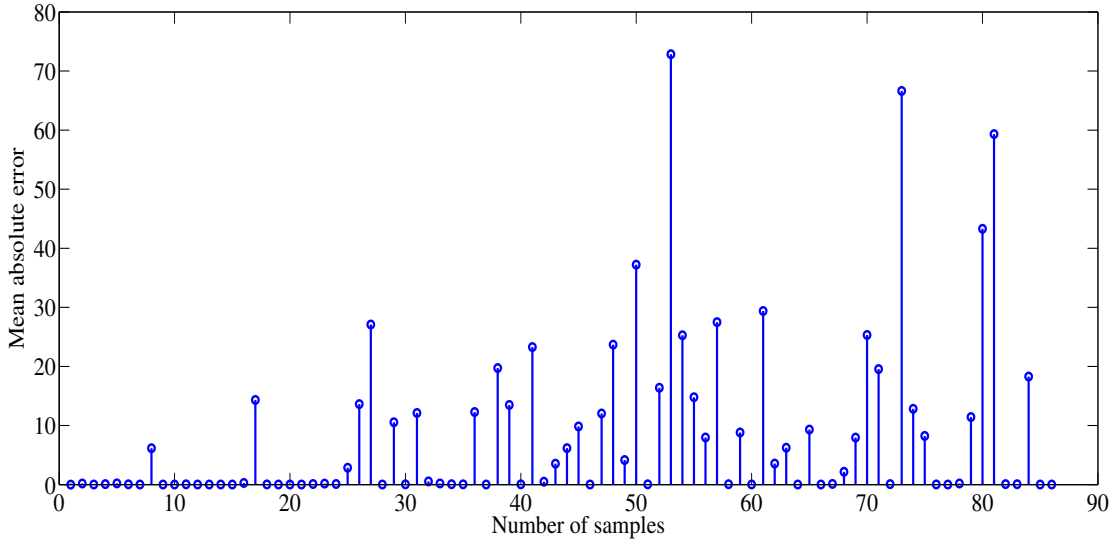

Figure 4.14: Mean absolute error of lunch event of days 1, 3 and 6.

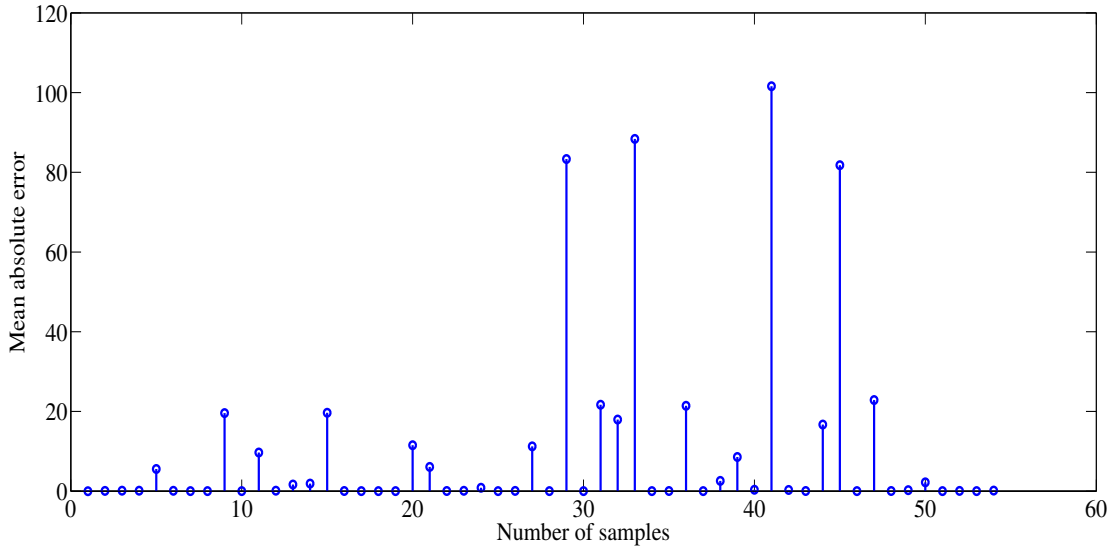

Figure 4.15: Mean absolute error of dinner event of days 2, 3 and 4.

Also, to have a look of the dispersion of the best sets of selected parameters, each of the parameters were normalized and then graphed in a boxplot. The central mark on the box indicates the median, and the bottom and top edges of the box indicate the 25th and 75th percentiles, respectively. These boxplots can be seen in Figures 4.16, 4.17 and 4.18.

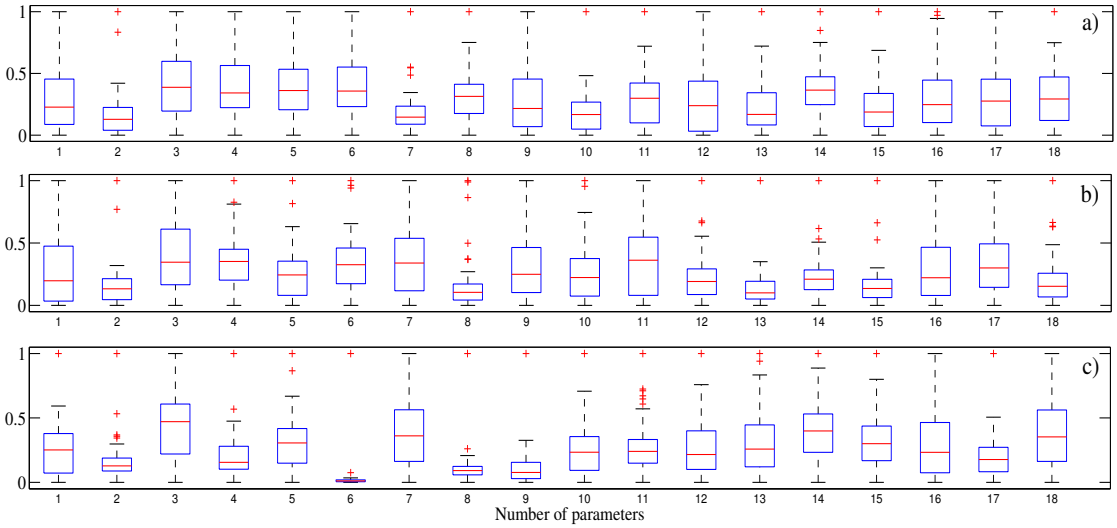

Figure 4.16: Boxplot of adjusted parameters of breakfast event for a) day 1, b) day 4 and c) day 6.

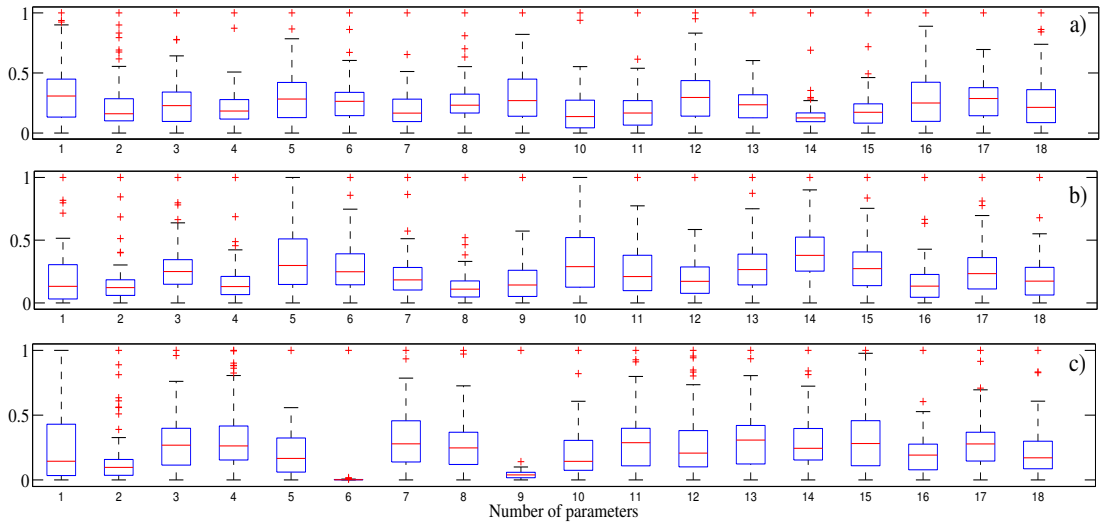

Figure 4.17: Boxplot of adjusted parameters of lunch event for a) day 1, b) day 3 and c) day 6.

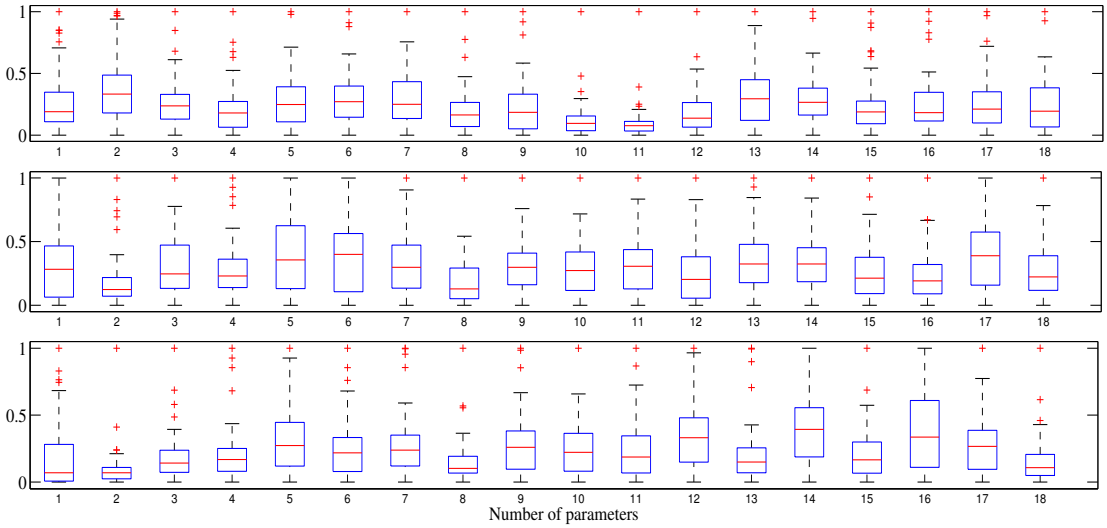

Figure 4.18: Boxplot of adjusted parameters of dinner event for a) day 2, b) day 3 and c) day 4.

4.5 Closed-loop control

As stated in Section 3, a proportional-integral-derivative (PID) controller was proposed in order to analyze the response of the physiological model for T2DM. The model was linearized around its equilibrium point, in order to get the state-space form to implement the PID controller. The matrices A, B, C and D from the linearization (using the model (3.8) - (3.29)) are as follows:

$$A_{1,j} = \begin{bmatrix} -2.29 & 0.61 & 1.68 & 0 & 0 & 0 & 0 & 0 & 0 & 0 & 0 & 0 & 0 & 0 & 0 & 0 & 0 & 0 & 0 & 0 & 0 & 0 \end{bmatrix}$$

$$A_{2,j} = \begin{bmatrix} 0.47 & -0.47 & 0 & 0 & 0 & 0 & 0 & 0 & 0 & 0 & 0 & 0 & 0 & 0 & 0 & 0 & 0 & 0 & 0 & 0 & 0 & 0 \end{bmatrix}$$

$$A_{3,j} = \begin{bmatrix} 0.42 & 0 & -3.16 & 0 & 0.91 & 0.73 & 1.09 & 0 & 0 & 0 & 0 & 0 & 0 & 0 & 0 & 0 & 0 & 0 & 0 & 0 & 0 & 0 \end{bmatrix}$$

$$A_{4,j} = \begin{bmatrix} 0 & 0 & 0.90 & -0.90 & 0 & 0 & 0 & 0 & 0 & 0 & 0 & 0 & 0 & 0 & 0 & 0 & 0 & 0 & 0 & 0 & 0 & 0 \end{bmatrix}$$

$$A_{5,j} = \begin{bmatrix} 0 & 0 & 0.09 & 0.4023 & -0.59 & 0 & 0 & 0 & 0 & 0 & 0 & 0 & 0 & 0 & 6.25 & -2.29 & -4.67 \\ 1.9 & 0 & 0 & 0 \end{bmatrix}$$

$$A_{6,j} = \begin{bmatrix} 0 & 0 & 1.53 & 0 & 0 & -1.53 & 0 & 0 & 0 & 0 & 0 & 0 & 0 & 0 & 0 & 0 & 0 & 0 & 0 & 0 & 0 \end{bmatrix}$$

$$A_{7,j} = \begin{bmatrix} 0 & 0 & 1.45 & 0 & 0 & 0 & -2.74 & 1.29 & 0 & 0 & 0 & 0 & 0 & 0 & 0 & 0 & 0 & 0 & 0 & 0 & 0 \end{bmatrix}$$

$$A_{8,j} = \begin{bmatrix} 0 & 0 & 0 & 0 & 0 & 0 & 0.20 & -0.20 & 0 & 0 & 0 & 0 & 0 & 0 & -0.015 & 0 & 0 & 0 & 0 & 0 & 0 \\ 0 \end{bmatrix}$$

$$A_{9,j} = \begin{bmatrix} 0 & 0 & 0 & 0 & 0 & 0 & 0 & 0 & -1.73 & 1.73 & 0 & 0 & 0 & 0 & 0 & 0 & 0 & 0 & 0 & 0 & 0 \end{bmatrix}$$

$$A_{10,j} = \begin{bmatrix} 0 & 0 & 0 & 0 & 0 & 0 & 0 & 0 & 0.45 & -3.15 & 0 & 0.90 & 0.72 & 1.06 & 0 & 0 & 0 & 0 & 0 & 0 \\ 0 & 0 \end{bmatrix}$$

$$A_{11,j} = \begin{bmatrix} 0 & 0 & 0 & 0 & 0 & 0 & 0 & 0 & 0 & 0.76 & -0.76 & 0 & 0 & 0 & 0 & 0 & 0 & 0 & 0 & 0 & 0 \end{bmatrix}$$

$$A_{12,j} = \begin{bmatrix} 0 & 0 & 0.05 & 0 & 0 & 0 & 0 & 0 & 0 & 0.09 & 0.37 & -0.78 & 0 & 0 & 0 & 0 & 0 & 0 & 0 & 0 & 0 \\ 0 & 0 \end{bmatrix}$$

$$A_{13,j} = \begin{bmatrix} 0 & 0 & 0 & 0 & 0 & 0 & 0 & 0 & 0 & 1.41 & 0 & 0 & -1.83 & 0 & 0 & 0 & 0 & 0 & 0 & 0 & 0 \end{bmatrix}$$

$$A_{14,j} = \begin{bmatrix} 0 & 0 & 0 & 0 & 0 & 0 & 0 & 0 & 0 & 1.41 & 0 & 0 & 0 & -1.87 & 0.45 & 0 & 0 & 0 & 0 & 0 & 0 \end{bmatrix}$$

$$A_{15,j} = \begin{bmatrix} 0 & 0 & 0 & 0 & 0 & 0 & 0 & 0 & 0 & 0 & 0 & 0 & 0 & 0.05 & -0.11 & 0 & 0 & 0 & 0 & 0 & 0 \end{bmatrix}$$

$$A_{16,j} = \begin{bmatrix} 0 & 0 & 0 & 0 & 0 & 0 & 0 & 0 & 0 & 0 & 0 & -0.0005 & 0 & 0 & 0 & -0.04 & 0 & 0 & 0 & 0 & 0 & 0 \end{bmatrix}$$

$$A_{17,j} = \begin{bmatrix} 0 & 0 & 0 & 0 & 0 & 0 & 0 & 0.001 & 0 & 0 & 0 & 0 & -0.04 & 0 & 0 & 0 & 0 & 0 \end{bmatrix}$$

$$A_{18,j} = \begin{bmatrix} 0 & 0 & 0 & 0 & 0 & 0 & 0 & 0 & 0 & 0 & 0 & 0 & 0 & 0 & 0 & 0 & 0 & -0.0154 & 0.003 & 0 & 0 & 0 \end{bmatrix}$$

$$A_{19,j} = \begin{bmatrix} 0 & 0 & -0.0007 & 0 & 0 & 0 & 0 & 0 & 0 & -0.04 & 0 & 0 & 0 & 0 & 0 & 0 & 0 & 0 & -0.09 & 0 & 0 \\ 0 \end{bmatrix}$$

$$A_{20,j} = \begin{bmatrix} 0 & 0 & -0.0001 & 0 & 0 & 0 & 0 & 0 & 0 & 0 & 0 & 0 & 0 & 0 & 0 & 0 & 0 & 0 & 0 & -0.01 & 0.095 \\ 0 \end{bmatrix}$$

$$A_{21,j} = \begin{bmatrix} 0 & 0 & 0.0001 & 0 & 0 & 0 & 0 & 0 & 0 & 0 & 0 & 0 & 0 & 0 & 0 & 0 & 0 & 0 & 0 & 0 & -0.04 & 0 \end{bmatrix}$$

$$A_{22,j} = \begin{bmatrix} 0 & 0 & 0.003 & 0 & 0 & 0 & 0 & 0 & 0 & 0 & 0 & 0 & 0 & 0 & 0 & 0 & 0 & 0 & 0 & 0 & 0 & -0.93 \end{bmatrix}$$

$$B = \begin{bmatrix} 0 & 0 & 0 & 0 & 0 & 0 & 0 & 0 & 0 & 0 & 0 & 0 & 0 & 0 & 0.148 & 0 & 0 & 0 & 0 & 0 & 0 & 0 \end{bmatrix}^T$$

$$C = \begin{bmatrix} 0 & 0 & 0 & 0 & 0 & 0 & 0 & 1 & 0 & 0 & 0 & 0 & 0 & 0 & 0 & 0 & 0 & 0 & 0 & 0 & 0 & 0 \end{bmatrix}$$

$$D = [0]$$

where $j = 22$ for matrix A. Figure 4.19 shows the implementation of the nonlin-

ear system in open-loop, and Figure 4.20 shows the implementation of the control scheme performed in Simulink®.

The PID controller was tuned using the *Tune* command from Simulink® . For this purpose the linearization of the physiological model, described in Subsection 3.1.1 was needed. The implementation was performed with the nonlinear system with nominal parameters as reported in Table 2.2.

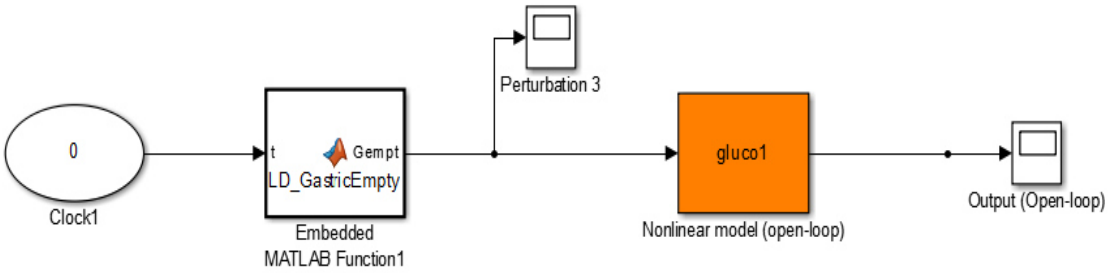

Figure 4.19: Open-loop implementation diagram in Simulink® of the physiological model.

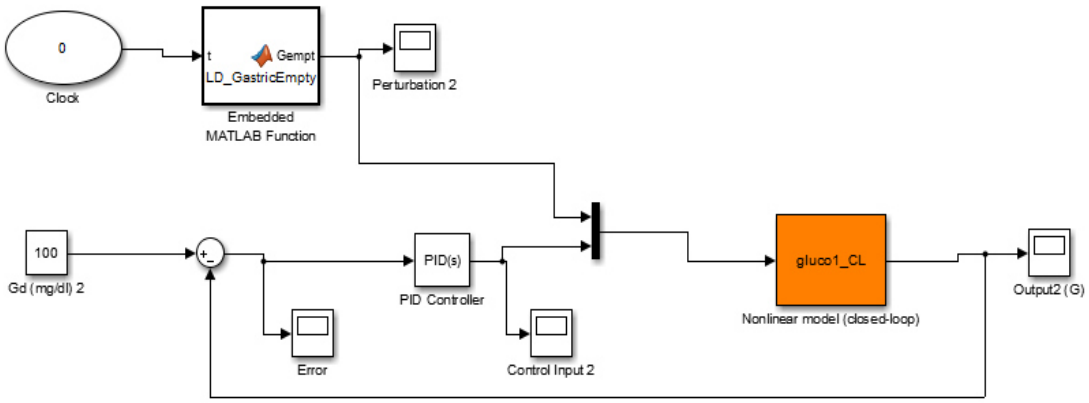

Figure 4.20: Closed-loop implementation diagram considering the PID tuned using the autotunning command of Simulink®

The controller scheme was proved with the three meals of the six days reported in the experimental study. This is shown in Figures 4.21 - 4.26, where the green band represents the normoglycemic range (70 *mg/dl* - 120 *mg/dl*).

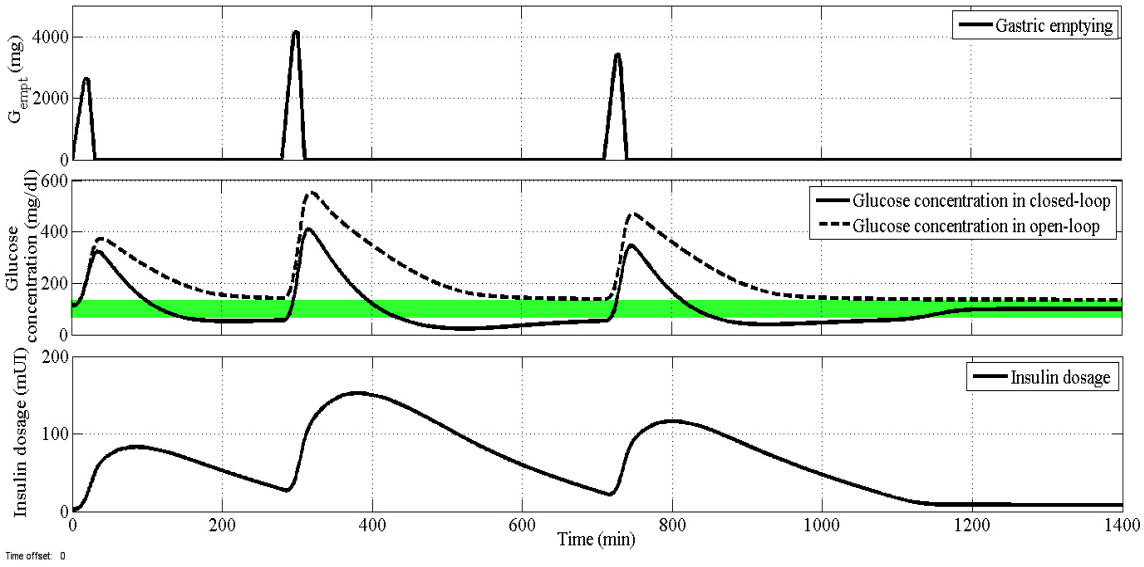

Figure 4.21: Control results for day 1 of the three meal simulation taken from the experimental set up, where the green band represents the normoglycemic range (70 *mg/dl* - 120 *mg/dl*).

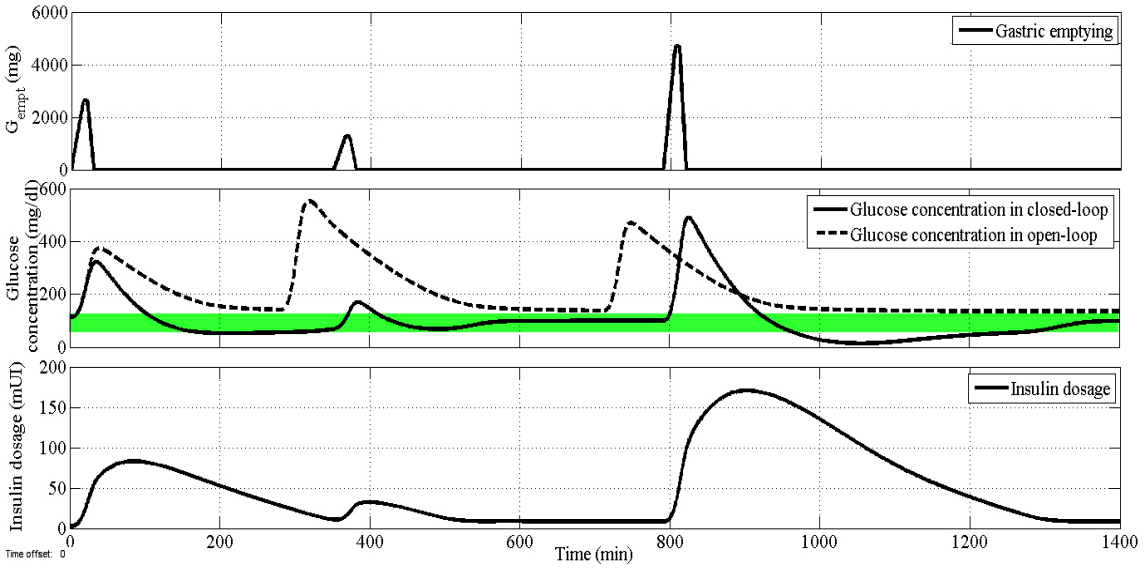

Figure 4.22: Control results for day 2 of the three meal simulation taken from the experimental set up, where the green band represents the normoglycemic range (70 *mg/dl* - 120 *mg/dl*).

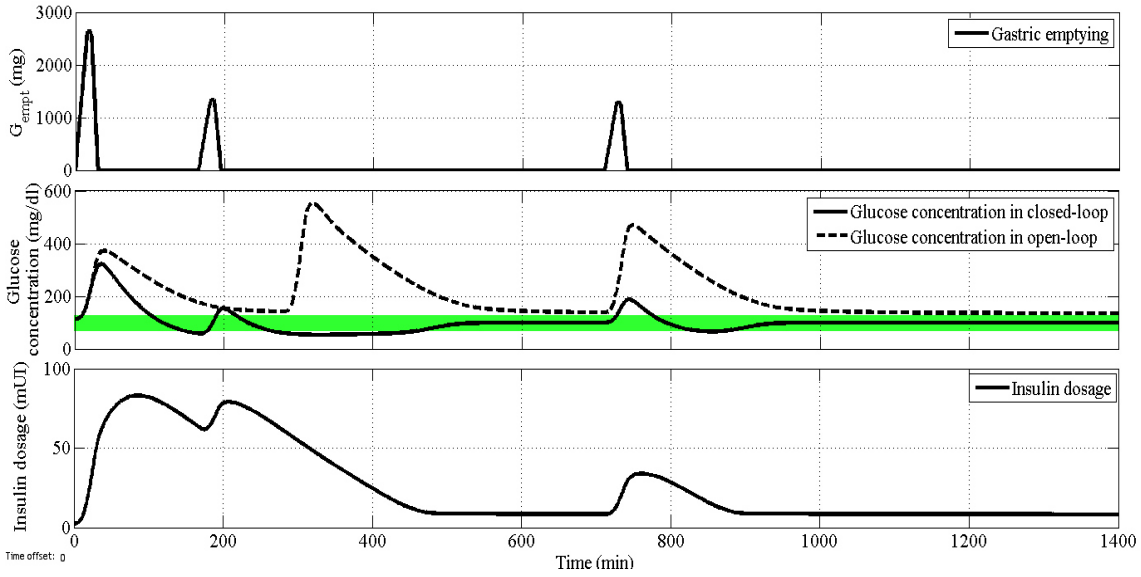

Figure 4.23: Control results for day 3 of the three meal simulation taken from the experimental set up, where the green band represents the normoglycemic range (70 *mg/dl* - 120 *mg/dl*).

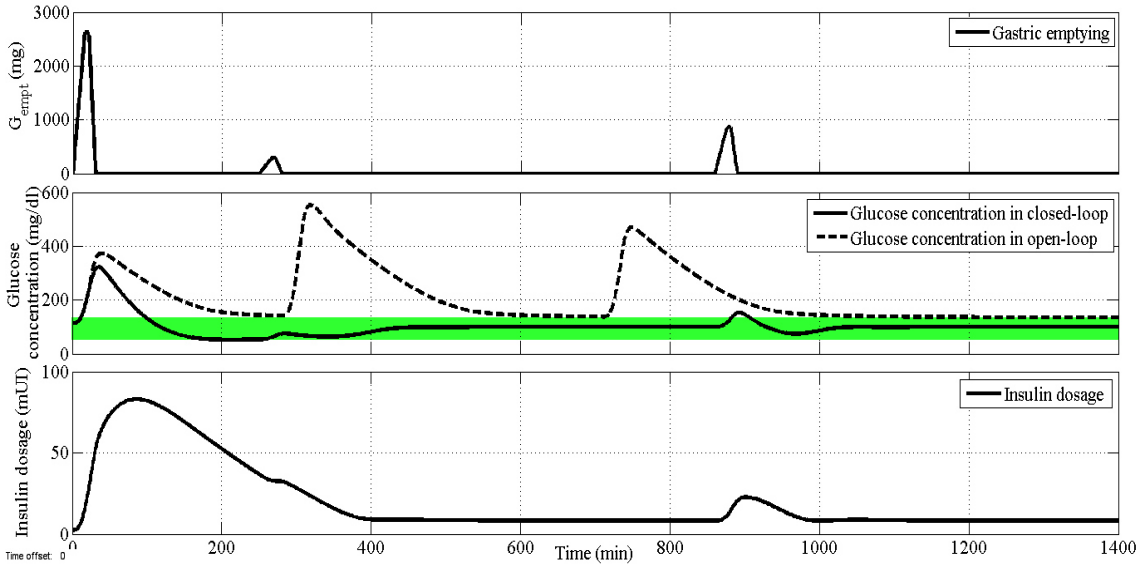

Figure 4.24: Control results for day 4 of the three meal simulation taken from the experimental set up, where the green band represents the normoglycemic range (70 *mg/dl* - 120 *mg/dl*).

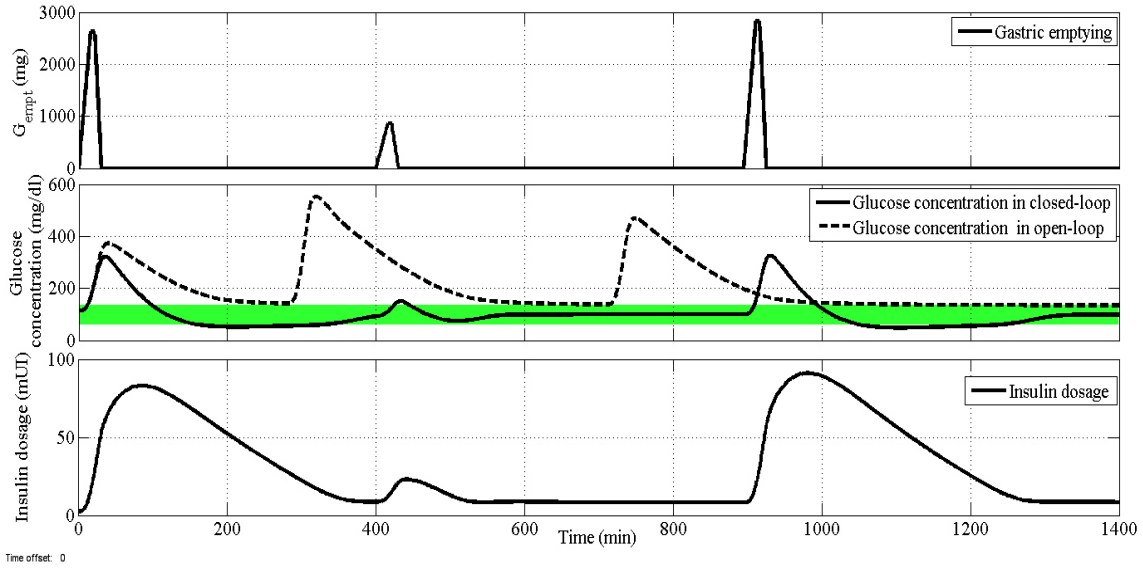

Figure 4.25: Control results for day 5 of the three meal simulation taken from the experimental set up, where the green band represents the normoglycemic range (70 *mg/dl* - 120 *mg/dl*).

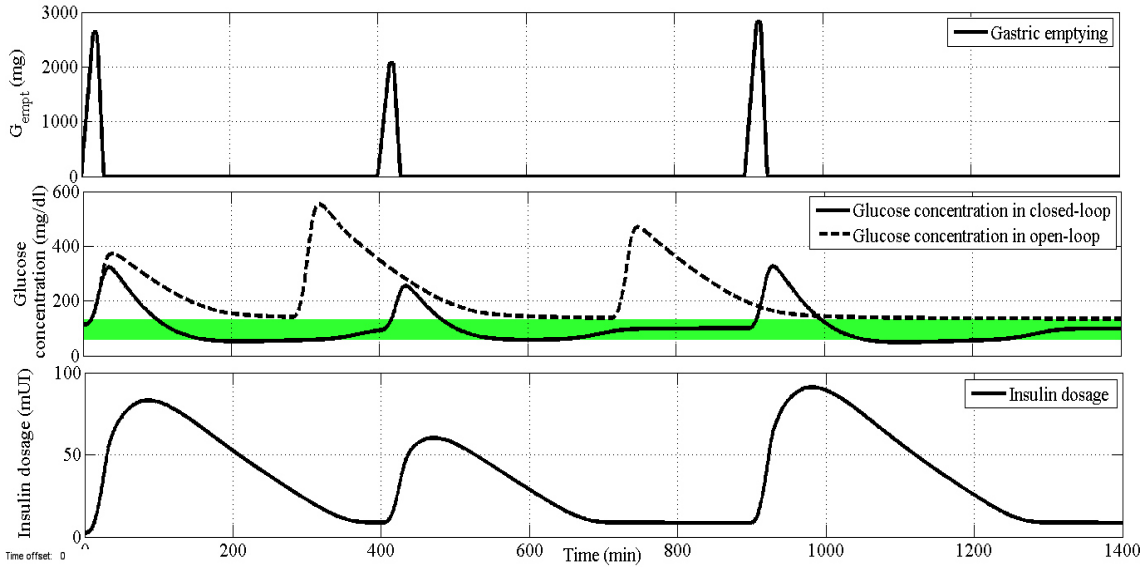

Figure 4.26: Control results for day 6 of the three meal simulation taken from the experimental set up, where the green band represents the normoglycemic range (70 *mg/dl* - 120 *mg/dl*).

Chapter 5

Conclusions and Future Work

After working with two different models of glucose-insulin dynamics, it was concluded that the most optimal model was the physiological model proposed by Vahidi *et al.* because of its robustness and detailed explanation of the interaction between organs. Conversely, the meal simulation model proposed by Dalla Man *et al.* can be an intuitive model but mathematically speaking, complications were presented when the parametric adjustment was tried to be made because of the non-linearity of the rate of glucose appearance. Similarly, observation issues were presented in the attempt of implementing the adaptive observer with the complete model.

The conclusion about the parameter and state estimation is that the adaptive observer was an adequate tool to solve this problem because of the nature of the process. As a future work, the full scheme is proposed, that is work with the complete meal-glucose-insulin model as a whole, instead of a cascade adaptation. The complete observance of the system is yet to be proved.

About the sensitivity analysis of the meal-glucose-insulin model, the resulting parameters were the expected ones because of the processes that they were involved in. Those parameters where chosen for the parametric adjustment, which results, as it was stated before, were not conclusive and most of the simulations took days to complete the computation. In reference of the physiological model,

the parametric adjustment had a good performance but the width of the windows samples were too small to actually work with the resulting parameters. Therefore, it is proposed to implement it with wider windows and more patient data.

In the work done with the control scheme, it was shown that the linearization is required to tune a conventional PID controller. Yet, there is a phase difference between the open-loop signal and the closed-loop signal of some simulations due to the controller. Therefore the linearization, as well as the controller, is an opportunity area to work with. While it is right that PID controllers are widely used in the industry, it was confirmed by the simulations that this scheme is not the most accurate to work with for blood glucose regulation.

Since the necessity of a control scheme for T2DM therapy is clear, and many methodologies can be improved to get better results in blood glucose regulation, it is proposed as a future work to develop a robust control scheme to have an automated therapy. Also, it is seek to modify the glucose metabolism model so that the effect of antihyperglycemic drugs can be added to the model, as well as exercise and insulin action. With altogether, it will be possible to start developing a methodology for *in silico* models in order to have a patient orientated model considering insulinization therapy. By having this tool it is expected to help improving T2DM therapy.

Bibliography

[1] International Diabetes Federation. Idf diabetes atlas, 7th edn., 2017.

[2] Instituto nacional de salud pública. Encuesta nacional de salud y nutrición de medio camino, 2016.

[3] Ishan Ajmera, Maciej Swat, Camille Laibe, Nicolas Le Novere, and Vijayalakshmi Chelliah. The impact of mathematical modeling on the understanding of diabetes and related complications. *CPT: pharmacometrics & systems pharmacology*, 2(7):1–14, 2013.

[4] Richard N Bergman, Y Ziya Ider, Charles R Bowden, and Claudio Cobelli. Quantitative estimation of insulin sensitivity. *American Journal of Physiology-Endocrinology And Metabolism*, 236(6):E667, 1979.

[5] A Bagust and S Beale. Deteriorating beta-cell function in type 2 diabetes: a long-term model. *Qjm*, 96(4):281–288, 2003.

[6] AM Albisser, Y Yamasaki, H Broekhuyse, and J Tiran. Hypercomplex models of insulin and glucose dynamics: Do they predict experimental results? *Annals of biomedical engineering*, 8(4-6):539–557, 1980.

[7] John Thomas Sorensen. *A physiologic model of glucose metabolism in man and its use to design and assess improved insulin therapies for diabetes*. PhD thesis, Massachusetts Institute of Technology, 1985.

[8] Karin Alvehag and Clyde Martin. The feedback control of glucose: on the road to type ii diabetes. In *Decision and Control, 2006 45th IEEE Conference on*, pages 685–690. IEEE, 2006.

[9] O Vahidi, KE Kwok, RB Gopaluni, and L Sun. Developing a physiological model for type ii diabetes mellitus. *Biochemical Engineering Journal*, 55(1):7–16, 2011.

[10] Hamed Abedini Najafabadi and Mohammad Shahrokhi. Model predictive control of blood sugar in patients with type-1 diabetes. *Optimal Control Applications and Methods*, 37(4):559–573, 2016.

[11] Joseph El Youssef, Jessica Castle, and W Kenneth Ward. A review of closed-loop algorithms for glycemic control in the treatment of type 1 diabetes. *Algorithms*, 2(1):518–532, 2009.

[12] Stamatina Zavitsanou, Athanasios Mantalaris, Michael C Georgiadis, and Efstratios N Pistikopoulos. In silico closed-loop control validation studies for optimal insulin delivery in type 1 diabetes. *IEEE Transactions on Biomedical Engineering*, 62(10):2369–2378, 2015.

[13] Chiara Dalla Man, Francesco Micheletto, Dayu Lv, Marc Breton, Boris Kovatchev, and Claudio Cobelli. The uva/padova type 1 diabetes simulator: new features. *Journal of diabetes science and technology*, 8(1):26–34, 2014.

[14] Boris P Kovatchev, Marc Breton, Chiara Dalla Man, and Claudio Cobelli. In silico preclinical trials: a proof of concept in closed-loop control of type 1 diabetes, 2009.

[15] Illinois Technology Institute. Glucosim: a web-based educational simulation package for glucose–insulin levels in human body [online].

[16] FDA. Artificial pancreas device system [online].

[17] Metronics Diabetes. Fda approves the minimed 670g system, world's first hybrid closed loop system [online].

[18] Brian Topp, Keith Promislow, Gerda Devries, Robert M Miura, and DIANE T FINEGOOD. A model of β-cell mass, insulin, and glucose kinetics: pathways to diabetes. *Journal of theoretical biology*, 206(4):605–619, 2000.

[19] Andrea De Gaetano and Ovide Arino. Mathematical modelling of the intravenous glucose tolerance test. *Journal of mathematical biology*, 40(2):136–168, 2000.

[20] Hanna E Silber, Petra M Jauslin, Nicolas Frey, Ronald Gieschke, Ulrika SH Simonsson, and Mats O Karlsson. An integrated model for glucose and insulin regulation in healthy volunteers and type 2 diabetic patients following intravenous glucose provocations. *The Journal of Clinical Pharmacology*, 47(9):1159–1171, 2007.

[21] O Vahidi, KE Kwok, R Bhushan Gopaluni, and FK Knop. A comprehensive compartmental model of blood glucose regulation for healthy and type 2 diabetic subjects. *Medical & biological engineering & computing*, 54(9):1383–1398, 2016.

[22] Nor Azlan Othman, Paul D Docherty, Nor Salwa Damanhuri, and J Geoffrey Chase. Tracking the progression to type 2 diabetes with a proportional-derivative insulin secretion model. *Control Engineering Practice*, 59:165–172, 2017.

[23] Filippo Amato, Alberto López, Eladia María Peña-Méndez, Petr Vaňhara, Aleš Hampl, and Josef Havel. Artificial neural networks in medical diagnosis, 2013.

[24] Oğuz Karan, Canan Bayraktar, Haluk Gümüşkaya, and Bekir Karlık. Diagnosing diabetes using neural networks on small mobile devices. *Expert Systems with Applications*, 39(1):54–60, 2012.

[25] Chongjian Wang, Linlin Li, Ling Wang, Zhiguang Ping, Muanda Tsobo Flory, Gaoshuai Wang, Yuanlin Xi, and Wenjie Li. Evaluating the risk of type 2 diabetes mellitus using artificial neural network: an effective classification approach. *Diabetes research and clinical practice*, 100(1):111–118, 2013.

[26] Alphus D Wilson and Manuela Baietto. Applications and advances in electronic-nose technologies. *Sensors*, 9(7):5099–5148, 2009.

[27] Ehab I Mohamed, R Linder, G Perriello, N Di Daniele, SJ Pöppl, and A De Lorenzo. Predicting type 2 diabetes using an electronic nose-based artificial neural network analysis. *Diabetes, nutrition & metabolism*, 15(4):215–221, 2002.

[28] Shin Hwa Lee and Kwang-il Kwon. Pharmacokinetic-pharmacodynamic modeling for the relationship between glucose-lowering effect and plasma concentration of metformin in volunteers. *Archives of pharmacal research*, 27(7):806–810, 2004.

[29] Lin Sun, Ezra Kwok, Bhushan Gopaluni, and Omid Vahidi. Pharmacokinetic-pharmacodynamic modeling of metformin for the treatment of type ii diabetes mellitus. *The open biomedical engineering journal*, 5:1, 2011.

[30] Sukankana Chakraborty, Kriti Arora, Prakash Kumar Sharma, Arijit Nath, and Chiranjib Bhattacharjee. Pharmacokinetics study of metformin–mathematical modelling and simulation. *APCBEE Procedia*, 9:151–158, 2014.

[31] UK Prospective Diabetes Study (UKPDS) Group et al. Intensive blood-glucose control with sulphonylureas or insulin compared with conventional treatment and risk of complications in patients with type 2 diabetes (ukpds 33). *The lancet*, 352(9131):837–853, 1998.

[32] Guo Lian, Xu Yue, Zhang Xianxiang, Luo Yong, Liu Weijuan, and Chen Bing. Insulinization: A promising strategy for the treatment of type 2 diabetes mellitus. *Experimental and therapeutic medicine*, 6(5):1300–1306, 2013.

[33] Roman Hovorka, Valentina Canonico, Ludovic J Chassin, Ulrich Haueter, Massimo Massi-Benedetti, Marco Orsini Federici, Thomas R Pieber, Helga C Schaller, Lukas Schaupp, Thomas Vering, et al. Nonlinear model predictive control of glucose concentration in subjects with type 1 diabetes. *Physiological measurement*, 25(4):905, 2004.

[34] Chiara Dalla Man, Robert A Rizza, and Claudio Cobelli. Meal simulation model of the glucose-insulin system. *IEEE Transactions on biomedical engineering*, 54(10):1740–1749, 2007.

[35] ED Lehmann and T Deutsch. A physiological model of glucose-insulin interaction in type 1 diabetes mellitus. *Journal of biomedical engineering*, 14(3):235–242, 1992.

[36] L Torres. Evonorm, a new evolutionary algorithm to continuous optimization. In *Workshop on Optimization by Building and Using Probabilistic Models (OBUPM 2006). Genetic and Evolutionary Computation Conference (GECCO 2006) CD Proceeding Tutorials and Workshops, Seattle*, 2006.

[37] Luis Torres-Trevino. Evonorm: Easy and effective implementation of estimation of distribution algorithms. *Special Issue: Advances in Computer Science and Engineering*, page 75, 2006.

[38] Harrison H Barrett, Jie Yao, Jannick P Rolland, and Kyle J Myers. Model observers for assessment of image quality. *Proceedings of the National Academy of Sciences*, 90(21):9758–9765, 1993.

[39] Deborah L Goldwasser. *Parameter estimation in mathematical models of lung cancer*. Rice University, 2010.

[40] Yoshito Hirata, Kai Morino, Taiji Suzuki, Qian Guo, Hiroshi Fukuhara, and Kazuyuki Aihara. System identification and parameter estimation in mathematical medicine: examples demonstrated for prostate cancer. *Quantitative Biology*, 4(1):13–19, 2016.

[41] Eugene Ackerman, Laël C Gatewood, John W Rosevear, and George D Molnar. Model studies of blood-glucose regulation. *Bulletin of Mathematical Biology*, 27:21–37, 1965.

[42] Richard N Bergman, Lawrence S Phillips, and Claudio Cobelli. Physiologic evaluation of factors controlling glucose tolerance in man: measurement of insulin sensitivity and beta-cell glucose sensitivity from the response to intravenous glucose. *Journal of clinical investigation*, 68(6):1456, 1981.

[43] F Stahl and Rolf Johansson. Short-term diabetes blood glucose prediction based on blood glucose measurements. In *Engineering in Medicine and Biology Society, 2008. EMBS 2008. 30th Annual International Conference of the IEEE*, pages 291–294. IEEE, 2008.

[44] Eleni I Georga, Vasilios C Protopappas, and Dimitrios I Fotiadis. Glucose prediction in type 1 and type 2 diabetic patients using data driven techniques. In *Knowledge-oriented applications in data mining*. InTech, 2011.

[45] Chiara Dalla Man, Michael Camilleri, and Claudio Cobelli. A system model of oral glucose absorption: validation on gold standard data. *IEEE Transactions on Biomedical Engineering*, 53(12):2472–2478, 2006.

[46] A Rodríguez, G Quiroz, R Femat, HO Méndez-Acosta, and J de León. An adaptive observer for operation monitoring of anaerobic digestion wastewater treatment. *Chemical Engineering Journal*, 269:186–193, 2015.

[47] Hassan K Khalil. Noninear systems. *Prentice-Hall, New Jersey*, 2(5):5–1, 1996.

[48] Edyta Cichocka, Anna Wietchy, Katarzyna Nabrdalik, and Janusz Gumprecht. Insulin therapy—new directions of research. *Endokrynologia Polska*, 67(3):314–324, 2016.

[49] Robyn Houlden, Stuart Ross, Stewart Harris, Jean-Francois Yale, Luc Sauriol, and Hertzel C Gerstein. Treatment satisfaction and quality of life using an early insulinization strategy with insulin glargine compared to an adjusted oral therapy in the management of type 2 diabetes: the canadian insight study. *Diabetes research and clinical practice*, 78(2):254–258, 2007.

[50] Itamar Raz and Ofri Mosenzon. Early insulinization to prevent diabetes progression. *Diabetes care*, 36(Supplement 2):S190–S197, 2013.

[51] Lin Sun, Ezra Kwok, Bhushan Gopaluni, and Omid Vahidi. A feedback glucose control strategy for type ii diabetes mellitus. In *Advanced Control of Industrial Processes (ADCONIP), 2011 International Symposium on*, pages 349–352. IEEE, 2011.

[52] F Ekram, L Sun, O Vahidi, E Kwok, and RB Gopaluni. A feedback glucose control strategy for type ii diabetes mellitus based on fuzzy logic. *The Canadian Journal of Chemical Engineering*, 90(6):1411–1417, 2012.

[53] National Instruments. Pid theory explained, 2011.

[54] José Manuel Zamora Martínez. Modulo didactico de control basado en lego mindstorms y simulink. Bachelor's thesis, Instituto Tecnológico Superior de Uruapan, 2017.

[55] G Quiroz and R Femat. On hyperglicemic glucose basal levels in type 1 diabetes mellitus from dynamic analysis. *Mathematical biosciences*, 210(2):554–575, 2007.

List of Figures

Appendix A: Academic productivity

During the course of this research the article entitled as "Parameter and state estimation of a mathematical model of carbohydrate intake" was presented in the 2^{nd} Conference on Modeling, Identification and Control of Nonlinear Systems (MICNON 2018) organized by the International Federation of Automatic Control (IFAC) in Guadalajara, Jalisco, Mexico, held from June 20^{th} to June 22^{th}.

Parameter and State Estimation of a Mathematical Model of Carbohydrate Intake ⋆

A. Olay-Blanco, A. Rodriguez-Liñan, G. Quiroz

Universidad Autónoma de Nuevo León, Facultad de Ingeniería Mecánica y Eléctrica, Av. Universidad S/N, Cd. Universitaria, San Nicolás de los Garza, N.L., C.P. 66455, México (e-mail: ana.olaybl, angel.rodriguezln, griselda.quirozcm{@uanl.edu.mx})

Abstract: Carbohydrate intake is one of the main disturbances in blood glucose metabolism and one of the major care-issues in diabetes therapy. For this reason, the dynamics of glucose absorption after a meal intake must be included in glucose metabolism models. Current interest in developing patient-specific models has shown the necessity to estimate key parameters in models of carbohydrate intake, which cannot be measured with available sensor technology. In this contribution, we present a scheme to estimate a parameter and a state related to absorption of glucose in the intestine, which depend on the amount of carbohydrates ingested in a meal. The scheme is based on an adaptive observer with exponential convergence to estimate states and uncertain constant parameters.

Keywords: Parameter estimation, patient-specific models, glucose metabolism modeling, carbohydrate intake, glucose dynamics.

1. INTRODUCTION

In 2015, the World Health Organization (WHO (2015)) disclosed the main diseases responsible for more than half of the worldwide deaths, situating diabetes on the 6th place. The latest statistics of the International Diabetes Federation (IDF (2017)) reported that there are 425 million people worldwide (between 20 and 79 years old) with some type of diabetes; and in 2045, this number could rise 627 million people. Type 2 diabetes mellitus (T2DM) is the one with more cases in the world, affecting about 87% to 91% of the diabetic patients.

Along with the right treatment to control the glycemic levels, lifestyle is important in diabetes care. Since energy is produced from glucose and the main way the body gathers it is by carbohydrate (CHO) intake, it is important to include nutritional therapy to bring blood glucose concentration into normoglycemic levels. There is an association between having a balanced diet (with the guidance of a dietitian) and a decrement of the percentage of glycosylated hemoglobin (HbA1C). Studies about the role of macronutrients in diabetic diet are not conclusive; but it has been demostrated that low-CHO diets reduce Hb1Ac about 0.2% to 0.5% (ADA (2017) and Wheeler et al. (2012)). Also, He et al. (2010) showed that including whole grains in diet is related with the decrement of cardiovascular diseases and mortality rate in diabetic patients. In some cases, T2DM patients can required insulin-based therapy; that is, daily insulin doses depending on their glycemic levels (Lian et al. (2013)). Conventionally doses are prescribed according to the clinical features of patients but their lifestyle habits (meal and exercise) are uncertain or unknown. Recent studies have shown that automation of insulin dosage could improve glucose management in diabetic patients (Riddle et al. (2003)). Such approach requires the mathematical modeling of the main processes related to glucose-insulin dynamics, including the glucose absorption from daily CHO intake. Mathematical modeling of glucose metabolism has had a major development in the last decades; including systemic models (Ackerman et al. (1965), Bergman et al. (1981)), black-box models (Stahl and Johansson (2008), Georga et al. (2011)), and compartmental models (Sorensen (1985), Hovorka et al. (2004)); but not all models are useful in solving the automation of insulin dosage.

An appropriated model for this end must consider the full-relationship from CHO intake to blood glucose concentration. Dalla Man et al. (2007) have contributed to solve this problem, they presented a model of glucose metabolism including meal dynamics; however, it depends on the rate of glucose appearance in the intestine (Ra), which is an unmeasured process. In insulin dosage automation, the only available measured variable is glucose concentration; therefore, the model proposed by Dalla Man et al. (2007) must be improved in order to provide the full-relationship from CHO intake to blood glucose concentration. For this reason, in this paper we propose an approach to estimate the rate of glucose appearance in the intestine; that is, a sensorless approach to know the effect of CHO intake in glucose metabolism. This idea is sketched in Fig. 1, we consider the gastric emptying model (Dalla Man et al. (2006)) which input is the CHO intake ($D\delta(t)$) and it computes the rate of glucose appearance in the intestine (Ra). In

⋆ G. Quiroz thanks the National Council of Science and Technology (CONACYT) for financial support (grant 220187). A. Olay-Blanco also thanks CONACYT for scholarship (grant 448599).

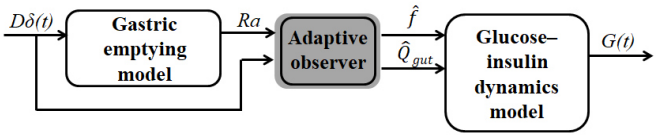

Fig. 1. Block diagram of the sensorless approach to include the effect of CHO intake in glucose-insulin metabolism models. An adaptive observer with exponential convergence is proposed to estimate the rate of glucose appearance in the intestine.

turn, Ra and $D\delta(t)$ are the inputs of the proposed adaptive observer, which is an state affine scheme with exponential convergence to estimate states and uncertain constant parameters. In this case, the observer estimates uncertain parameter f and the state related to mass of glucose in the intestine (Q_{gut}), both from the gastric emptying model. Once the parameter and the state are estimated, the effect of CHO intake can be included in the glucose-insulin metabolism model, which output is the measured blood glucose concentration ($G(t)$). This paper is organized as follows: Section 2 presents the methodologies to model gastric emptying and glucose-insulin metabolism. The proposed scheme to estimate a parameter and the states of the gastric emptying model is outlined in Section 3. The numerical implementation of the estimation scheme and the main results are in Section 4. Finally, a brief discussion and some concluding remarks are in Section 5.

2. MODELING METHODOLOGIES

To model the full-relationship from CHO intake to blood glucose concentration we used the previous approaches reported by Dalla Man *et al.*: one for the gastric emptying process after a CHO intake (Dalla Man et al. (2006)), and other one for glucose-insulin metabolism (Dalla Man et al. (2007)). As it was discussed in the Introduction section, the problem of the gastric emptying model is that it includes an uncertain parameter (f), which is related to the amount of ingested CHO. Therefore the design of the adaptive observer is based on such model that is described in subsection 2.1. Once the rate of glucose appearance is estimated, the effect of the CHO intake in the glucose-insulin metabolism can be illustrated using the model proposed by Dalla Man et al. (2007), which is described in subsection 2.2.

2.1 Gastric emptying model

Gastric emptying in the human body regulates the glucose uptake. After the stomach is emptied, all of the absorbed material goes into the intestines, this has been proved by some studies where the glucose absorption in the small intestine is considerated as a nonlinear process (Marathe et al. (2013)). Lehmann and Deutsch (1992) presented a physiological model of glucose and insulin interaction in type 1 diabetic patients. They described glucose uptake in the gut by considering that the amount of glucose (represented in grams of CHO) is being absorbed at a certain rate. Also the stomach is getting emptied according to the quantity of the ingested CHO. The proposed gastric emptying curve was set to be a triangular function if the ingestion was less than 10 g of CHO or a trapezoidal function if it was greater or equal than 10 g of CHO. Recently, Yokrattanasak et al. (2016) considered gastric emptying as an irregular process by modeling the transition from the full stomach to the duodenum and the jejunum. This process was proposed to be a stochastic model where the meal in the stomach at time t_0 is 100%, and the gastric emptying is done by random releases (spurts) until the matter in stomach approaches to zero. Thus, the sequence of spurts can be used as input in a glucose-insulin metabolism model.

Regarding the physiological modeling approach, Dalla Man et al. (2006) proposed two models for oral glucose absorption based on Ra data previously recorded in experiments. Those models describe the transit of CHO intake in three phases: two phases for the transit through the stomach, and one for the transit in the intestines. The main difference between both models was the way the gastric rate was described; in one model it is stated as a linear function and in the other as a nonlinear one, where the latter fits better Ra data. For this reason, in this paper we use the second model and it is described below:

$$\frac{dQ_{sto1}(t)}{dt} = -k_{gri}Q_{sto1}(t) + D\delta(t) \quad (1)$$

$$\frac{dQ_{sto2}(t)}{dt} = -k_{empt}(Q_{sto})Q_{sto2}(t) + k_{gri}Q_{sto1}(t) \quad (2)$$

$$\frac{dQ_{gut}(t)}{dt} = -k_{abs}Q_{gut}(t) + k_{empt}(Q_{sto})Q_{sto2}(t) \quad (3)$$

where $Q_{sto1}(t)$ (mg) and $Q_{sto2}(t)$ (mg) are the glucose masses in the stomach for both phases, $Q_{gut}(t)$ (mg) is the glucose mass in the intestine, k_{abs} (min^{-1}) is the constant rate of intestinal absorption, k_{gri} is the rate of grinding, D (mg) is the amount of CHO intake, $\delta(t)$ is an impulse function because the response time of the glucose metabolism is higher than the response time of the food intake and it is widely used in literature. The rate of gastric emptying $k_{empt}(Q_{sto})$ describes the transit of the total mass of glucose in the stomach into the intestine, starting at a maximum rate k_{max} (min^{-1}) at the beginning of the transit and decreasing to a minimum rate k_{min} (min^{-1}), by the function:

$$\begin{aligned} k_{empt}(Q_{sto}) = k_{min} + \frac{k_{max} - k_{min}}{2} \\ * \{tanh\left[\frac{5}{2D(1-b)}(Q_{sto}(t) - bD)\right] \\ - tanh\left[\frac{5}{2Dc}(Q_{sto}(t) - cD)\right] + 2\} \end{aligned} \quad (4)$$

where $Q_{sto}(t) = Q_{sto1}(t) + Q_{sto2}(t)$ is the total amount of glucose in the stomach (mg), b and c are the percentages of the dose for which k_{empt} decreases and rises back to $(k_{max} - k_{min})/2$, respectively. The rate of glucose appearance depends on the final absorption by the intestine:

$$Ra(t) = \frac{fk_{abs}Q_{gut}(t)}{BW} \quad (5)$$

where f (dimensionless) is the fraction of intestinal absorption that actually appears in plasma and BW is the body weight (kg). As it can be verified, parameter f depends

on Ra data involving an experimental protocol which is no feasible in insulin dosage automation, where the only no-invasive measure is blood glucose concentration.

2.2 Glucose-insulin metabolism model

As it was stated before, it is necessary to have a model that describes the glucose-insulin dynamics. Here we present the model proposed by Dalla Man et al. (2007), which is divided in five subsystems. The first one is the glucose subsystem, which describes the mass of glucose in plasma and rapidly equilibrating tissues ($G_p(t)$) and the mass of glucose in slowly equilibrating tissues ($G_t(t)$). This subsystem takes endogenous ($EGP(t)$) and exogenous ($Ra(t)$) sources of glucose, as well as the insulin-dependent ($U_{id}(t)$) and -independent ($U_{ii}(t)$) glucose utilization and renal excretion ($E(t)$):

$$\frac{dG_p(t)}{dt} = EGP(t) + Ra(t) - U_{ii}(t) - E(t) - k_1 G_p(t) + k_2 G_t(t) \quad (6)$$

$$\frac{dG_t(t)}{dt} = -U_{id}(t) + k_1 G_p(t) - k_2 G_t(t) \quad (7)$$

where k_1 and k_2 (min^{-1}) are the rate parameters of distribution. The blood glucose concentration $G(t)$ is the relationship of appearance of the mass of glucose in plasma $G_p(t)$ in a certain distribution volume V_G, this is described as follows:

$$G(t) = \frac{Gp(t)}{V_G} \quad (8)$$

The second subsystem describes the mass of the insulin in liver ($I_l(t)$) and in blood ($I_p(t)$):

$$\frac{dI_l(t)}{dt} = -(m_1 + m_3(t))I_l(t) + m_2 I_p(t) + S(t) \quad (9)$$

$$\frac{dI_p(t)}{dt} = -(m_2 + m_4)I_p(t) + m_1 I_l(t) \quad (10)$$

where m_1, m_2, $m_3(t)$, m_4 (min^{-1}) are rate parameters of distribution and $S(t)$ (pmol/L/min) is the insulin secretion. The blood insulin concentration $I(t)$ can be described in a similar way than blood glucose concentration, where the plasmatic mass I_p of insulin is delivered within a distribution volume V_I, this process is described as follows:

$$I(t) = \frac{Ip(t)}{V_I} \quad (11)$$

The endogenous source of glucose, $EGP(t)$ is described by the third subsystem:

$$\frac{dI_d(t)}{dt} = -k_i[I_d(t) - I_1(t)] \quad (12)$$

$$\frac{dI_1(t)}{dt} = -k_i[I_1(t) - I(t)] \quad (13)$$

where $I_d(t)$ is a delayed insulin signal, $I_1(t)$ is an auxiliary variable of $I_d(t)$ and k_i (min^{-1}) is the rate parameter accounting for delay between insulin signal and insulin action. The fourth subsystem is the glucose utilization ($X(t)$):

$$\frac{dX(t)}{dt} = -p_{2U}X(t) + p_{2U}[I(t) - I_b] \quad (14)$$

where I_b (pmol/L) is the basal insulin concentration and p_{2U} ($\text{min}^{-}1$) is the rate constant of insulin action of the peripheral glucose utilization.

Finally, the last subsystem describes insulin secretion:

$$\frac{dI_{po}(t)}{dt} = -\gamma I_{po}(t) + S_{po}(t) \quad (15)$$

$$\frac{dY(t)}{dt} = \begin{cases} -\alpha[Y(t) - \beta(G(t) - h)], \\ \text{if } \beta(G(t) - h) \geq -S_b \\ -\alpha Y(t) - \alpha S_b, \\ \text{if } \beta(G(t) - h) < -S_b \end{cases} \quad (16)$$

where $I_{po}(t)$ stands for the insulin in portal vein and $Y(t)$ is the insulin release threshold. γ (min^{-1}) is the transfer rate constant between portal vein and liver, h (mg/dl) is the threshold level of glucose above which β-cells initiate to produce new insulin, α (min^{-1}) is the delay between glucose signal and insulin secretion, β (pmol/kg/min) is the pancreatic responsivity to glucose, $S_{po}(t)$ (pmol/L/min) is the insulin secretion of the portal vein and S_b is the basal insulin secretion.

3. ESTIMATION IN GLUCOSE-INSULIN METABOLISM

Estimation is a helpful tool in the biomedical field because of the lack of sensors to measure many physiological signals. An example of this is in mathematical modeling, where it is necessary to have enough sensed data to validate the models. Numerous applications of mathematical observers or estimators can be found in many areas in order to overcome the lack of sensors; for example Barrett et al. (1993) optimized the quality of a medical image by identifying a weak signal in a noisy picture. That was done by the implementation of a mathematical observer including the ideal Bayesian, nonprewhitening filter and a Hotelling observer. In the oncology field, Goldwasser (2010) proposed a method to estimate the lung cancer risk due to repeated low-dose of radiation exposures. Also a statistical approach to understand the natural course of lung cancer was proposed there. Another application in oncology is the work by Hirata et al. (2016), where a parametric estimation problem in a model of androgen deprivation treatment on prostate cancer was resolved. They proposed two solutions: cross entropy and the Bayesian theorem, both approaches were resolved using available patient data.

There is many work to be done to estimate physiological variables or parameters in mathematical models of glucose metabolism; because most of the metabolic processes cannot be measured or their measurement involves clinical procedures or invasive methods. Regarding gastric emptying model, for example the model presented by Dalla Man et al. (2006) has the disadvantage that the parameter f is uncertain. Moreover, in Dalla Man et al. (2007), the

glucose metabolism model includes such gastric emptying model, and thus Ra and f are both unknown. Thus, we present a preliminary estimation of parameter f for the gastric emptying model of Dalla Man et al. (2006).

3.1 Design of an adaptive observer

In this work, the parameter f is estimated using the adaptive observer proposed by Rodríguez et al. (2015), which was used in a cascade system of anaerobic digestion for wastewater. For estimation purposes, the process model must be structured as the following state affine system:

$$\begin{cases} \dot{x} = A(y,u)\,x + \beta(y,u) + \varphi(y,u)\,\theta \\ \quad\quad + Bg(y,u,x,\theta) \\ y = Cx \end{cases} \tag{17}$$

where $x \in \Re^n$ is the state vector, $\theta \in \Re^q$ is the unknown constant parameter vector, $u \in \Re^l$ is the input vector, $y \in \Re^r$ is the measurable output. $A(y,u)$, $\beta(y,u)$, $\varphi(y,u)$, $g(y,u,x,\theta)$, B and C are matrices of appropriate dimensions. Furthermore, n, q, l and r are the state space, parameter space, control space, and output space dimensions of system (17), respectively.

Considering that $A(y,u)$, $\beta(y,u)$, $\varphi(y,u)$ and $g(y,u,x,\theta)$ satisfy the Assumptions A1-A3 from Rodríguez et al. (2015), an adaptive observer for (17) is given by:

$$\begin{cases} \dot{\hat{x}} = A(y,u)\,\hat{x} + \beta(y,u) + \varphi(y,u)\,\hat{\theta} + Bg(y,u,\hat{x},\hat{\theta}) \\ \quad\quad + \{S_L^{-1}C^T + \Lambda\Gamma^{-1}\Lambda^T C^T\}Q(y - C\hat{x}) \\ \dot{S}_L = -\rho S_L - A^T(y,u)\,S_L - S_L A(y,u) + C^T QC \\ \dot{\Lambda} = \{A(y,u) - S_L^{-1}C^T QC\}\Lambda + \varphi(y,u) \\ \dot{\Gamma} = -\lambda\Gamma + \Lambda^T C^T QC\Lambda \\ \dot{\hat{\theta}} = \Gamma^{-1}\Lambda^T C^T Q(y - C\hat{x}) \end{cases} \tag{18}$$

where $\hat{x}$ and $\hat{\theta}$ are estimations of x and θ, respectively. The parameters $\rho \in \Re$ and $\lambda \in \Re$ modify the gains $S_L \in \Re^{n\times n}$, $\Lambda \in \Re^{n\times q}$ and $\Gamma \in \Re^{q\times q}$, of the observer for n states, l inputs, r outputs and q unknown parameters. $Q \in \Re^{r\times r}$, S_L and Γ are positive definite symmetric matrices. The exponential convergence proof of the adaptive observer (18) to system (17) is demonstrated in Rodríguez et al. (2015). By means of some algebraic manipulation, the system (1)-(5) can be written as (17) with:

$$x = \begin{bmatrix} x_1 \\ x_2 \\ x_3 \end{bmatrix} = f \begin{bmatrix} Q_{sto1}(t) \\ Q_{sto2}(t) \\ Q_{gut}(t) \end{bmatrix} \tag{19}$$

$$\theta = f, \quad u = D\delta(t), \quad y = Ra(t),$$

$$A(y,u) = \begin{bmatrix} -k_{gri} & 0 & 0 \\ k_{gri} & -k_{max} & 0 \\ 0 & k_{max} & -k_{abs} \end{bmatrix},$$

$$\beta(y,u) = \begin{bmatrix} 0 \\ 0 \\ 0 \end{bmatrix}, \quad \varphi(y,u) = \begin{bmatrix} D\delta(t) \\ 0 \\ 0 \end{bmatrix},$$

$$B = \begin{bmatrix} 0 \\ -\dfrac{(k_{max} - k_{min})}{2} \\ \dfrac{(k_{max} - k_{min})}{2} \end{bmatrix},$$

$$g(y,u,x,\theta) = [\tanh(w) - \tanh(v)]\,x_2,$$

$$w = \frac{5(x_1 + x_2)}{2Df(1-b)} - \frac{5b}{2(1-b)},$$

$$v = \frac{5(x_1 + x_2)}{2Dcf} - \frac{5}{2},$$

$$\text{and} \quad C = \begin{bmatrix} 0 & 0 & \dfrac{k_{abs}}{BW} \end{bmatrix}.$$

Then, the adaptive observer (18) and the scalar mapping (19) allow the estimation of $\hat{Q}_{sto1}(t)$, $\hat{Q}_{sto2}(t)$, $\hat{Q}_{gut}(t)$ and $\hat{f}$ of the states $Q_{sto1}(t)$, $Q_{sto2}(t)$, $Q_{gut}(t)$ and parameter f, respectively; if the next assumptions hold:

(i) The system (1)-(3) is completely observable.
(ii) The Assumptions A1-A3 from Rodríguez et al. (2015) are satisfied.

Then, the estimation of $Ra(t)$ is computed as

$$\hat{Ra}(t) = \frac{k_{abs}\hat{x}_3}{BW}. \tag{20}$$

4. NUMERICAL IMPLEMENTATION AND RESULTS

The proposed scheme is given by equations of the original model (1)-(3), and the adaptive observer defined in (18). The numerical implementation of the whole system was coded in MATLAB® using the differential equation solver *ode45*. The simulation time was $t \in [0, 4000]$ minutes, and the vector of initial conditions for the model was $x_0 = [0\ 0\ 0]^T$, since the CHO intake is made in fasting conditions, this is when the stomach is empty, the initial conditions for the gastric emptying model were stated in zero.

To obtain acceptable results three meals were considered in the numerical implementation, as described in Fig. 2. Each meal was considered as the perturbation performed by $D\delta(t)$ was modeled as a train of five square pulses, with period of 6 minutes, giving a total of 30 minutes of CHO intake (see Fig. 2).

In order to illustrate the convergence of the estimated states, three different sets of initial conditions were arbitrarily stated as $\hat{x}_1(0) = \hat{x}_2(0) = \hat{x}_3(0) = 3\text{x}10^5$, $\hat{x}_1(0) = \hat{x}_2(0) = \hat{x}_3(0) = 4\text{x}10^5$ and $\hat{x}_1(0) = \hat{x}_2(0) = \hat{x}_3(0) = 9\text{x}10^5$ considering the initial condition for the estimated parameter as $\hat{f}(0) = 0.5$, $S_L(0) = [I] \in \Re^{3\times 3}$, $\Lambda(0) = \Gamma(0) = 1$.

Table 1. Parameter nominal values of the model and adaptive observer proposed by Dalla Man et al. (2007).

Parameter	Value
k_{gri}	0.0558 min^{-1}
k_{max}	0.0558 min^{-1}
k_{min}	0.008 min^{-1}
k_{abs}	0.057 min^{-1}
D	78000 mg
b	0.82
c	0.00236 mg^{-1}
BW	78 kg
f	1.2723
ρ	0.0710
λ	2

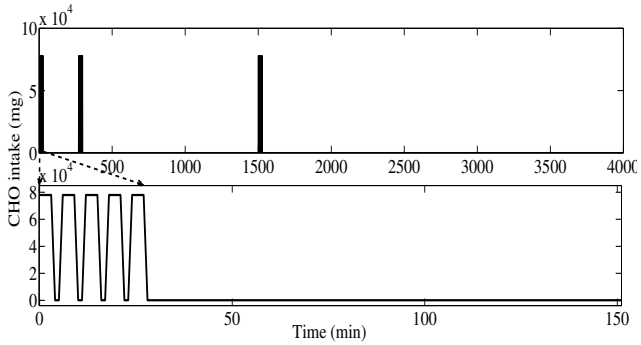

Fig. 2. CHO intake is modeled by $D\delta(t)$ as a train of five square pulses, with period of 6 minutes, giving a total of 30 minutes per meal. The disturbance is presented in the full simulation time (top), and a zoom in of a single meal is also included (bottom).

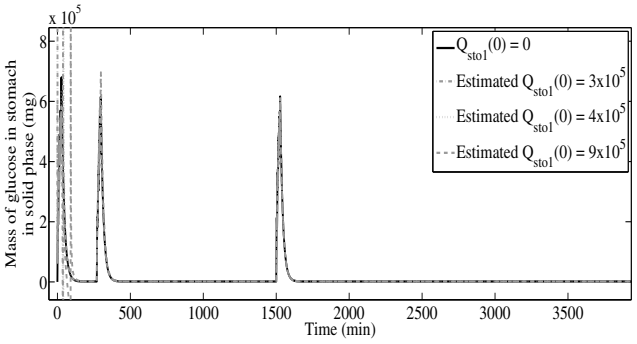

Fig. 3. Estimation of the glucose mass in solid phase, Q_{sto1}.

The nominal values of parameter of the model (1)-(3) are reported in Table 1, as well as the gains of the adaptive observer. The estimation of states can be verified in Fig. 3 - 5.

Moreover, the convergence of the estimated parameter $\hat{f}$ is shown in Fig. 6, considering three different initial conditions chosen as $\hat{f}(0) = 0.25$, $\hat{f}(0) = 0.5$ and $\hat{f}(0) = 3$. The resulting estimation of Ra is shown in Fig. 7. In all these figures, the original (solid line) and estimated (dash line) value are presented.

5. DISCUSSION AND CONCLUDING REMARKS

The proposed scheme provides a sensorless solution by the estimation of parameter f and state Q_{gut}. Since the

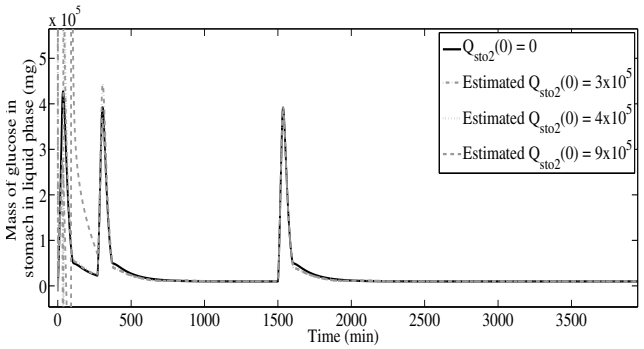

Fig. 4. Estimation of the glucose mass in liquid phase, Q_{sto2}.

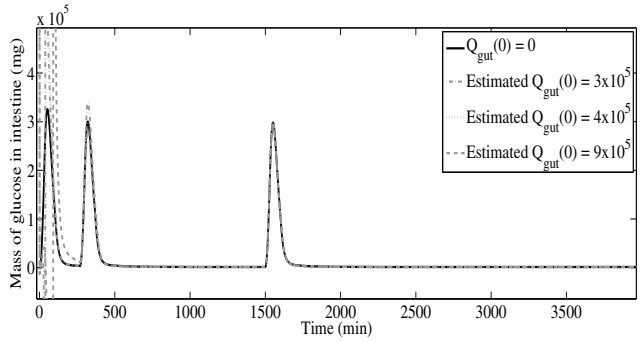

Fig. 5. Estimation of the glucose mass in the intestine, Q_{gut}.

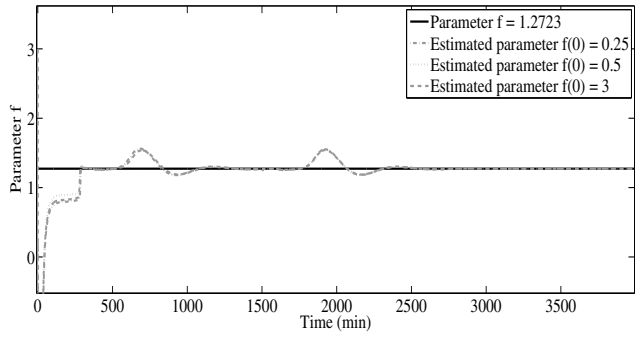

Fig. 6. Estimation of the uncertain parameter f involved in modeling of rate of glucose rate appearance, Ra.

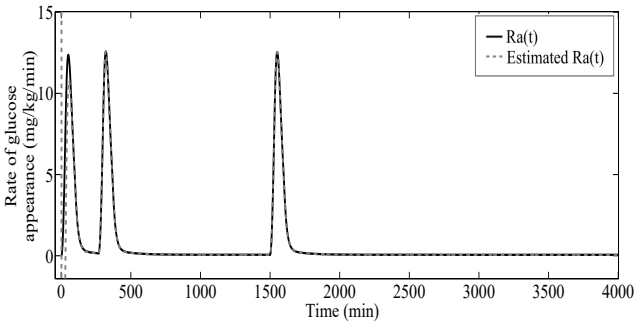

Fig. 7. Estimated vs original value of rate of glucose rate appearance, Ra.

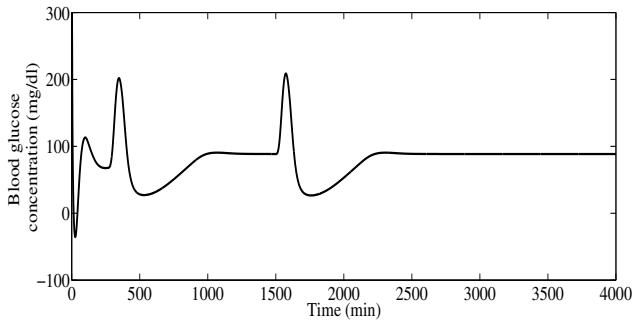

Fig. 8. Effect of the estimated disturbance in the glucose-insulin metabolism model by CHO intake.

observer has a convergence period, the simulation was made considering a typical 3-meal plan as shown in Fig. 2. The asymptotic convergence of the observer is illustrated in Fig. 3 - Fig. 7; there we can see that the scheme only required the time of one meal to be calibrated. In terms of glucose-insulin metabolism dynamics this calibration time is suitable. Regarding the estimation error, it is neglected after the calibration period. Blood glucose concentration after a meal can be properly reproduced by the glucose-insulin metabolism model only if Ra data is available, which is an unmeasured variable. Once the parameter f and state Q_{gut} are estimated, then we have an estimation of Ra (Fig. 7) to be used in the glucose-insulin metabolism model, and reproduce the effect of a CHO intake $D\delta(t)$ in the blood glucose concentration $G(t)$ (Fig. 8). In both cases, the estimation error is also neglected after the calibration period. In conclusion, we show that the adaptive observer provides a suitable solution to estimate unmeasured processes as the rate of glucose appearance. Thus, the scheme in Fig. 1 can be a mathematical approach to represent the full-relationship from CHO intake to blood glucose concentration, and in consequence, it could be a useful model to solve the automation of insulin dosage in T2DM treatment.

REFERENCES

Ackerman, E., Gatewood, L. C., Rosevear, J. W., Molnar, G. D., 1965. Model studies of blood-glucose regulation. Bulletin of Mathematical Biology 27, 21–37.

ADA, 2017. Lifestyle management. sec. 4. in standards of medical care in diabetes 2017. Diabetes Care 40 (1), S33–S43.

Barrett, H. H., Yao, J., Rolland, J. P., Myers, K. J., 1993. Model observers for assessment of image quality. Proceedings of the National Academy of Sciences 90 (21), 9758–9765.

Bergman, R. N., Phillips, L. S., Cobelli, C., 1981. Physiologic evaluation of factors controlling glucose tolerance in man: measurement of insulin sensitivity and beta-cell glucose sensitivity from the response to intravenous glucose. Journal of clinical investigation 68 (6), 1456.

Dalla Man, C., Camilleri, M., Cobelli, C., 2006. A system model of oral glucose absorption: validation on gold standard data. IEEE Transactions on Biomedical Engineering 53 (12), 2472–2478.

Dalla Man, C., Rizza, R. A., Cobelli, C., 2007. Meal simulation model of the glucose-insulin system. IEEE Transactions on biomedical engineering 54 (10), 1740–1749.

Georga, E. I., Protopappas, V. C., Fotiadis, D. I., 2011. Glucose prediction in type 1 and type 2 diabetic patients using data driven techniques. In: Knowledge-oriented applications in data mining. InTech.

Goldwasser, D. L., 2010. Parameter estimation in mathematical models of lung cancer. Rice University.

He, M., van Dam, R. M., Rimm, E., Hu, F. B., Qi, L., 2010. Whole-grain, cereal fiber, bran, and germ intake and the risks of all-cause and cardiovascular disease–specific mortality among women with type 2 diabetes mellitus. Circulation 121 (20), 2162–2168.

Hirata, Y., Morino, K., Suzuki, T., Guo, Q., Fukuhara, H., Aihara, K., 2016. System identification and parameter estimation in mathematical medicine: examples demonstrated for prostate cancer. Quantitative Biology 4 (1), 13–19.

Hovorka, R., Canonico, V., Chassin, L. J., Haueter, U., Massi-Benedetti, M., Federici, M. O., Pieber, T. R., Schaller, H. C., Schaupp, L., Vering, T., et al., 2004. Nonlinear model predictive control of glucose concentration in subjects with type 1 diabetes. Physiological measurement 25 (4), 905.

IDF, 2017. Idf diabetes atlas 8th edn. International Diabetes Federaration. Brussels, Belgium.

Lehmann, E., Deutsch, T., 1992. A physiological model of glucose-insulin interaction in type 1 diabetes mellitus. Journal of biomedical engineering 14 (3), 235–242.

Lian, G., Yue, X., Xianxiang, Z., Yong, L., Weijuan, L., Bing, C., 2013. Insulinization: A promising strategy for the treatment of type 2 diabetes mellitus. Experimental and therapeutic medicine 6 (5), 1300–1306.

Marathe, C. S., Rayner, C. K., Jones, K. L., Horowitz, M., 2013. Relationships between gastric emptying, postprandial glycemia, and incretin hormones. Diabetes Care 36 (5), 1396–1405.

Riddle, M. C., Rosenstock, J., Gerich, J., 2003. The treat-to-target trial. Diabetes care 26 (11), 3080–3086.

Rodríguez, A., Quiroz, G., Femat, R., Méndez-Acosta, H., de León, J., 2015. An adaptive observer for operation monitoring of anaerobic digestion wastewater treatment. Chemical Engineering Journal 269, 186–193.

Sorensen, J. T., 1985. A physiologic model of glucose metabolism in man and its use to design and assess improved insulin therapies for diabetes. Ph.D. thesis, Massachusetts Institute of Technology.

Stahl, F., Johansson, R., 2008. Short-term diabetes blood glucose prediction based on blood glucose measurements. In: Engineering in Medicine and Biology Society, 2008. EMBS 2008. 30th Annual International Conference of the IEEE. IEEE, pp. 291–294.

Wheeler, M. L., Dunbar, S. A., Jaacks, L. M., Karmally, W., Mayer-Davis, E. J., Wylie-Rosett, J., Yancy, W. S., 2012. Macronutrients, food groups, and eating patterns in the management of diabetes. Diabetes care 35 (2), 434–445.

WHO, 2015. The top 10 causes of death. World Health Organization.

Yokrattanasak, J., De Gaetano, A., Panunzi, S., Satiracoo, P., Lawton, W. M., Lenbury, Y., 2016. A simple, realistic stochastic model of gastric emptying. PloS one 11 (4), e0153297.